

AD-A037 469

GENERAL DYNAMICS/CONVAIR SAN DIEGO CALIF
COMPUTATIONAL RESEARCH ON INVISCID, UNSTEADY, TRANSONIC FLOW OV--ETC(U)
JAN 77 R J MAGNUS
CASD/LVP-77-010

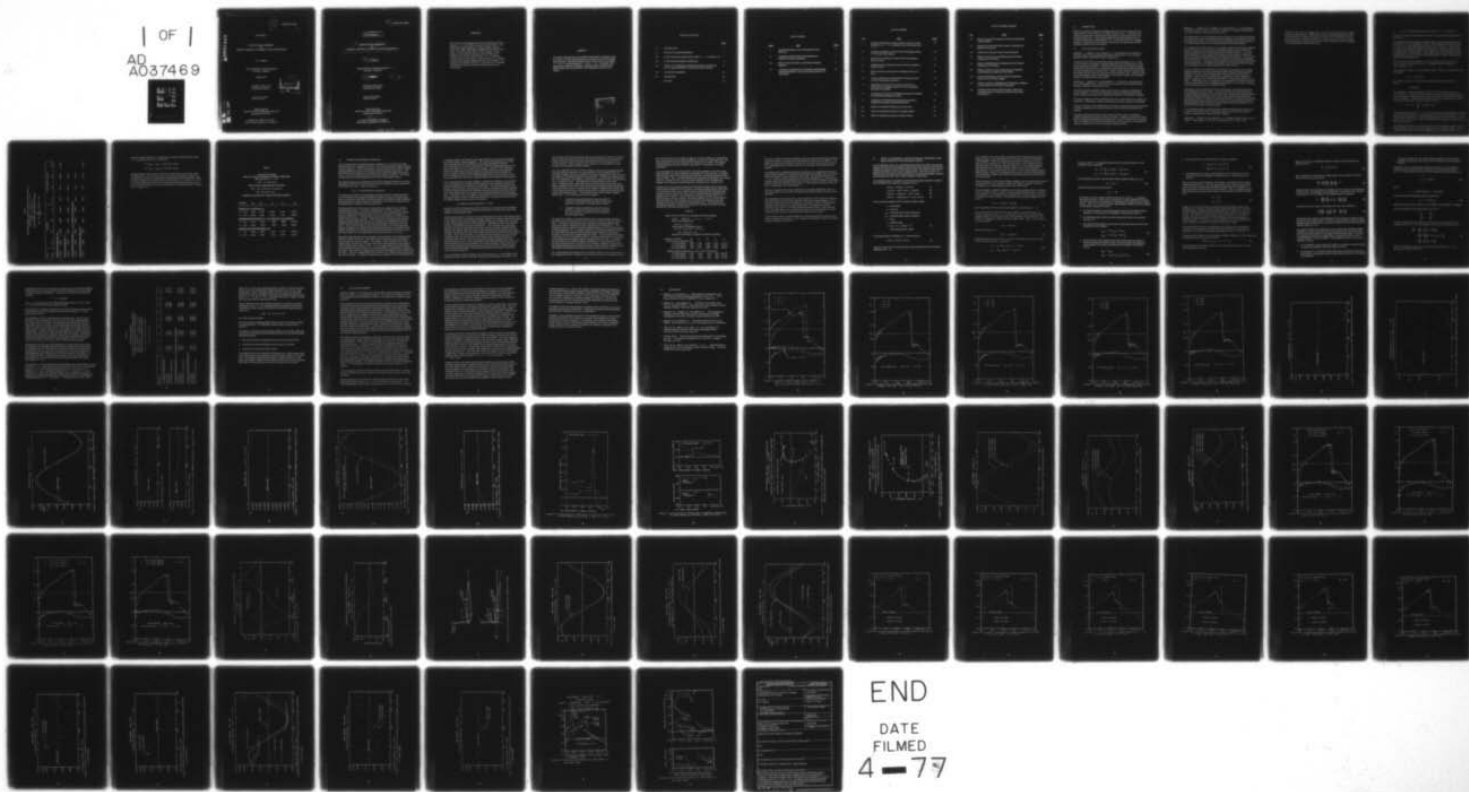
F/G 20/4

N00014-73-C-0294

NL

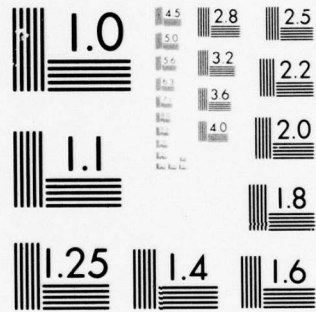
UNCLASSIFIED

| OF |
AD
A037469



END

DATE
FILMED
4 - 77



MICROCOPY RESOLUTION TEST CHART
NATIONAL BUREAU OF STANDARDS-1963-A

12

CASD/LVP 77-010

[Handwritten signature]

Final Report

COMPUTATIONAL RESEARCH
ON
INVISCID, UNSTEADY, TRANSONIC FLOW OVER AIRFOILS

R. J. Magnus

Convair Division of General Dynamics
San Diego, California

January 1977

Reproduction in whole or in part
is permitted for any purpose of
the United States Government.

D D C
MAR 28 1977
RESOLVED
[Handwritten initials]

Approved for public Release
Distribution Unlimited.

Sponsored by the
OFFICE OF NAVAL RESEARCH (Code 438)
Department of the Navy

Contract No. N00014-73-C-0294
ONR Contract Authority No. NR 061-214

AD A037469

AD NO. _____
DDC FILE COPY

14

CASD/LVP-77-010

9 Final Report,

6 COMPUTATIONAL RESEARCH ON INVISCID, UNSTEADY, TRANSONIC FLOW OVER AIRFOILS.

10 R. J. Magnus

Convair Division of General Dynamics /convair San Diego, California

11 January 1977

12 76 p.

Reproduction in whole or in part is permitted for any purpose of the United States Government.

Approved for public Release Distribution Unlimited.

Sponsored by the OFFICE OF NAVAL RESEARCH (Code 438) Department of the Navy

15 Contract No. N00014-73-C-0294 ONR Contract Authority No. NR 061-214

147 650

NT

FOREWORD

This research was undertaken by the Convair Division of General Dynamics, P. O. Box 80847, San Diego, California 92138. The work was done under the Office of Naval Research, Contract N00014-73-C-0294, ONR Contract Authority NR 061-214/12-07-72 (438). The ONR scientific officer was Mr. Ralph D. Cooper, Director, Fluid Dynamics Programs and the monitor of the technical effort was Mr. Morton Cooper. Dr. H. Yoshihara served as principal investigator at Convair and Dr. R. J. Magnus carried out the computer programming and the calculations. The assistance and cooperation of Dr. H. Lomax and Dr. W. Ballhaus, Fluid Dynamics Branch at NASA Ames Research Center are acknowledged.

ABSTRACT

The inviscid transonic flow over an NACA 64A410 airfoil oscillating in pitch in a Mach 0.72 stream was calculated with a program based on the unsteady Euler equations. The airfoil oscillates about a mid-chord axis with attitude $\alpha = 1^\circ \pm 1^\circ$ at reduced frequency $k \equiv \omega C/U_\infty = 0.2$. The effects of two approximations made in the analysis, handling boundary conditions at the airfoil surface and at the perimeter of the computation field, have been studied.

ACCESSION FOR	
DTIC	WORLD WIDE <input checked="" type="checkbox"/>
DDC	DDC <input type="checkbox"/>
UNANNOUNCED	<input type="checkbox"/>
JUSTIFICATION	
BY	
CLASSIFICATION/AVAILABILITY CODE	
DECL.	AVAIL. STATE/STANDARD
A	

TABLE OF CONTENTS

	<u>Page</u>
1.0 INTRODUCTION	1
1.1 NOTES ON THE REPORTS ISSUED	1
2.0 FLOW OVER 64A410 OSCILLATING ABOUT $\alpha = 1^\circ$ AT MACH 0.72	4
3.0 OUTER FIELD BOUNDARY CONDITIONS	8
4.0 EFFECT OF TRANSFER OF AIRFOIL BOUNDARY CONDITIONS TO THE MEAN POSITION OF THE OSCILLATING AIRFOIL	13
5.0 CONCLUDING REMARKS	22
6.0 REFERENCES	25
FIGURES	26

LIST OF TABLES

<u>Table</u>	<u>Title</u>	<u>Page</u>
I	Calculated Response, 64A410 Oscillating in Pitch, Mach 0.72	5
II	Comparison of Results With Two Amplitude and Reference Attitude Combinations	7
III	Effect of Outer Field Size on Calculated Oscillatory Response	11
IV	Comparison of Results From Calculations With Boundary Conditions Satisfied at Nodes on the Moving Airfoil or at Fixed Nodes	20

LIST OF FIGURES

<u>No.</u>	<u>Title</u>	<u>Page</u>
1	Pressure Distributions on NACA 64A410 in Mach 0.72 Flow; Steady Flow at $\alpha = 0, 2$ and Mean Value in Oscillation about $\alpha = 1$.	26
2.	Pressure Distributions on NACA 64A410 Oscillating in Mach 0.72 Flow (12 Phase Angles)	27
3.	Normal Force Coefficient on NACA 64A410 Oscillating in Mach 0.72 Flow	31
4.	Pitching Moment Coefficient on NACA 64A410 Oscillating in Mach 0.72 Flow	32
5.	Shock Location on NACA 64A410 Oscillating in Mach 0.72 Flow	33
6.	Pressure Coefficient on NACA 64A419 Oscillating in Mach 0.72 (5 Airfoil Surface Locations)	34
7.	Distribution of Excursions in Pressure Coefficient on NACA 64A410 Oscillating in Mach 0.72 Flow (Amplitudes and Phase Lead Angles)	38
8.	Comparison of Normal Force Responses Expected in Bounded and Unbounded Computational Fields	40
9.	Comparison of Pitching Moment Responses Expected in Bounded and Unbounded Computational Fields	41
10.	Effect of Computation Field Size on Normal Force	42
11.	Effect of Computation Field Size on Pitching Moment	43
12.	Effect of Computation Field Size on Shock Location	44

LIST OF FIGURES (continued)

<u>No.</u>	<u>Title</u>	<u>Page</u>
13.	Effect of Computation Field Size on Pressure Distribution (4 Phase Angles)	45
14.	Pressures in Outer Field (Mean Values, Amplitudes and Phases of Excursions)	49
15.	Airfoil-Fixed and Space-Fixed Coordinate System	51
16.	Effect on Normal Force of Satisfying Airfoil Boundary Conditions at Fixed Nodes	52
17.	Effect on Pitching Moment of Satisfying Airfoil Boundary Conditions at Fixed Nodes	53
18.	Effect on Position of Lower Surface Shock of Satisfying Airfoil Boundary Conditions at Fixed Nodes	54
19.	Pressure Distribution on NACA 64A010 Oscillating in Mach 0.80 Flow (6 Phase Angles)	55
20.	Effect on Pressure of Satisfying Airfoil Boundary Conditions at Fixed Nodes (5 Airfoil Surface Locations)	61
21.	Pressure Distributions on NACA 64A010 in Mach 0.80 Flow (Mean Values, Amplitudes and Phase Lead Angles of Excursions)	66

1.0 INTRODUCTION

Research on numerical solutions of unsteady transonic flows over airfoils has been conducted under Contract N00014-73-C-0294 since March 1972. During the course of the contract there have been four antecedent reports or papers issued which are discussed briefly below. These reports primarily deal with unsteady flows over the NACA 64A410 airfoil at Mach number 0.72. In this (final) report, an additional example is presented and two questions concerning effects of approximate handling of boundary conditions have been studied.

1.1 Notes on the Reports Issued

Reference 1. Magnus, R. and Yoshihara, H., "Finite Difference Calculations of the NACA 64A410 Airfoil Oscillating Sinusoidally In Pitch at $M_\infty = 0.72$ ", General Dynamics Convair, CASD-NSC-74-004, 1 August 1974.

The flow over the airfoil was calculated at three reduced frequencies, 0.2, 1.0 and 5.0, and results are presented in diagrams showing pressure distributions at various angles through the oscillations. The behavior of the pressures at selected locations on the airfoil, the shock waves, and the normal force and pitching moment coefficients are shown throughout the oscillation cycle. Simple "printer graphics" diagrams show the isobars near the airfoil at several points in the oscillation cycle. Except for statement of the equations used, the descriptions of the numerical method are not detailed and there is little discussion of the results.

Reference 2. Magnus, R. J. and Yoshihara, H., "Calculations of Transonic Flow Over an Oscillating Airfoil", AIAA Paper 75-98, 13th Aerospace Sciences Meeting, Pasadena, California, January 20-22, 1975.

The data on the three oscillatory cases covered in the first paper were digested by Fourier analysis. The forces and moments, pressures at selected airfoil surface points, and the shock location were inspected for evidence of non-sinusoidal response.

The isobar patterns around the oscillating airfoil were carefully drawn on a cathode-ray tube device. Additionally, contours showing rate-of-pressure change were generated.

A 16mm motion picture film showing the airfoil surface pressures and the isobar patterns about the oscillating airfoil (reduced frequency 0.20) was prepared and shown at the meeting.

The paper has some descriptions of the method of solution, notes on assumptions utilized, and the effort necessary to obtain a solution. Although it was explicitly stated that the method was **not** intended for production use, the fact that seven hours of computer time were spent on one solution has been quoted by a number of authors to advertise, by contrast, the efficiency of other subsequently developed methods.

Reference 3. Ballhaus, W. F., Magnus, R., and Yoshihara, H., "Some Examples of Unsteady Transonic Flows Over Airfoils", Symposium on Unsteady Aerodynamics, University of Arizona, Tucson, March 18-20, 1975.

In this paper there are short descriptions of two methods for calculating unsteady transonic flows over airfoils; the method based on the unsteady Euler equations used in the work described in Papers 1 and 2, and a method by Ballhaus and Lomax based upon a low frequency approximation to the transonic perturbation potential equation.

The response of the 64A410 airfoil to a step change in angle-of-attack from two degrees up to four degrees in Mach 0.72 flow (as calculated using the Euler equations) was examined in somewhat more detail than had been presented in Paper 2. There are figures showing the airfoil pressure distributions at specific times in the transient and histories of the surface pressures at six airfoil surface locations. These results were interpreted in a qualitative discussion mentioning waves and pulses originating at the airfoil surface. An omission which should be noted is that the initial part of the transient airfoil lift is reasonably well predicted by the linearized method of Heaslet, Lomax and Spreiter given in NACA Report 956 (or NACA TN1767).

There is a discussion of the difficulties of "tailoring" the parameters in a computer program based on the transonic perturbation potential equation (satisfying boundary conditions on a slit) so that the results match results calculated using the Euler equations. This discussion is illustrated by comparisons of results obtained for steady flow fields over the 64A410 airfoil at Mach 0.72 and angles-of-attack of 0° , 2° and 4° . Additionally, there is a comparison of unsteady flows calculated with the two methods for the 64A410 airfoil oscillating in pitch between 0° and 4° about a midchord axis at reduced frequency of 0.2 in Mach 0.72 flow.

Unfortunately, these comparisons of the two unsteady flow calculations did not show very satisfactorily similar results. Comments and criticisms accumulated since the paper appeared would seem to indicate that (a) the tailoring used in the perturbation program was too unsophisticated for the overly severe problem being attempting, (b) the Euler solution is probably not a good approximation to a physical flow (at flight Reynolds numbers) on a problem as severe as this one, (c) the ultimate usefulness of the perturbation method to calculate a broad range of unsteady flow problems is not disproved by the results on this one example.

It is noted that obtaining a solution with the perturbation method requires only about 1/30th as much computer time as obtaining a solution to this particular unsteady example with the program based on the Euler equations.

Reference 4. Magnus, R. and Yoshihara, H., "Unsteady Transonic Flows over an Airfoil", AIAA Journal, Vol. 13, No. 12, December 1975, pp. 1622 - 1628.

This paper is the result of rewriting Paper 2 to conform with requirements for publication in the archival journal. It differs from Paper 2 in having eliminated most of the isobar plots and by inclusion of an explicit presentation of the equations being solved. The text was heavily modified to clarify certain points and to answer questions raised by reviewers, and to put the material into forms which seemed to be more conventional for the presentation of unsteady airfoil data.

2.0 FLOW OVER 64A410 OSCILLATING ABOUT $\alpha = 1^\circ$ AT MACH 0.72

The flow over the NACA 64A410 in Mach number 0.72 flow had been studied earlier in References 1 - 4.

The example at reduced frequency 0.2 had the airfoil oscillating in pitch about a mid-chord axis $\pm 2^\circ$ from 2° mean angle-of-attack. This example has been characterized as overly severe because the peak Mach numbers at, for example, 4° angle-of-attack are over 1.6 and could not be achieved in an experiment. Therefore, a less severe example has been calculated using the same airfoil and the same computer program as was utilized in the cited references. This example has the 64A410 in Mach 0.72 flow oscillating in pitch about a mid-chord axis with amplitude $\pm 1^\circ$ about 1° mean angle-of-attack at reduced frequency 0.2.

The steady-flow pressure distributions at 0° and 2° angle-of-attack are shown in Figure 1, reproduced from earlier work. The highest local Mach number at 2° angle-of-attack is 1.42.

In the oscillatory example, the airfoil angle-of-attack, in degrees, was assumed to vary sinusoidally.

$$\alpha(t) = 1.0 + \sin(\omega t)$$

The circular frequency is related to the (non-dimensional) reduced frequency as follows:

$$\omega = kU_\infty/\text{chord}$$

The instantaneous pressure distributions at 30° intervals through an oscillation are shown in Figure 2. The histories of normal force, pitching moment about the quarter chord, shock location and the pressures at several locations on the airfoil are shown in Figures 3 through 6. Selected oscillatory data were fitted with approximating functions with (up to) four harmonics by a least squares procedure:

$$f(t) = B_0 + \sum_{n=1}^4 A_n \sin(n\omega t + \phi_n)$$

These data are listed in Table I. It may be seen by comparing the amplitudes of the higher harmonics with the amplitudes of the fundamentals that no great error would be realized if the traces were regarded as sinusoidal (except for pressures at stations traversed by the shock). This is also evident in Figures 5 and 6d where the light lines are the least-squares fitted single harmonics.

The chordwise distributions of the mean pressure coefficient during the oscillation and the first harmonic amplitudes and phase angles are shown in Figures 1 and 7. The distributions of amplitudes of the pressure oscillations are compared with quasi-steady

Table I

Calculated response, 64A410 oscillating in pitch, Mach 0.72

Mid-chord axis $\alpha = 1 \pm 1$ $k = 0.2$

$$\alpha(t) = \alpha_0 + \tilde{\alpha} \sin(\omega t)$$

Four harmonic representation of response:

$$f(t) = B_0 + \sum_{n=1}^4 A_n \sin(n\omega t + \phi_n)$$

Mean	Amplitudes				Phase Angles, Degrees			
B_0	A_1	A_2	A_3	A_4	ϕ_1	ϕ_2	ϕ_3	ϕ_4

Normal Force Coefficient, C_N

0.84449 .13175 .00087 .00009 .00003 -22.48 73.38 -169.49 134.04

Axial Force Coefficient, C_x

-.00281 .00533 .00024 .00001 .00000 142.77 106.44 -51.64 -

Pitching Moment Coefficient, C_m C/4 reference, nose up positive

-.15769 .01209 .00077 .00005 .00000 173.74 -9.95 74.62 -

Location of Upper Surface Shock, x/C

0.65711 .02809 .00150 .00015 .00002 -30.14 57.83 177.56 64.52

pressure changes obtained for 1.0 degree angle-of-attack excursions about a mean $\alpha = 1.0$ degree; the latter were calculated as:

$$0.5 (C_{p_{\alpha=2}} - C_{p_{\alpha=0}}) \text{ on the lower surface}$$

$$0.5 (C_{p_{\alpha=0}} - C_{p_{\alpha=2}}) \text{ on the upper surface}$$

Comparing these unsteady results with earlier results obtained on the same airfoil oscillating with $\alpha = 2 \pm 2^\circ$, it may be seen in Table II that the oscillatory parts of C_N are practically identical when normalized by the pitching oscillation amplitude. Since the shock is further forward (closer to the quarter chord) at $\alpha = 1^\circ$ than at $\alpha = 2^\circ$, and it was noted, (Reference 4) that about 0.8 of the pitching moment comes from shock motion at reduced frequency 0.2, the oscillatory part of the pitching moment is smaller at $\alpha = 1^\circ$ than at $\alpha = 2^\circ$.

Table II

Comparison of Results
 With Two Amplitude and Reference Attitude Combinations
 Mid-chord Axis $k = 0.2$

$$\alpha(t) = \alpha_0 + \tilde{\alpha} \sin(\omega t)$$

Single Harmonic Representation of Response

$$f(t) = B_0 + S_1 \sin(\omega t) + C_1 \cos(\omega t)$$

$$= B_0 + A_1 \sin(\omega t + \phi_1)$$

Responses normalized, per radian of oscillation amplitude

Function	B_0	S_1	C_1	A_1	ϕ_1
<u>Normal Force Coefficient, C_{N-}</u>					
$\alpha = 1 \pm 1$.8445	6.976	-2.884	7.549	-22.46
$\alpha = 2 \pm 2$	1.0521	6.831	-2.873	7.411	-22.81
<u>Pitching Moment Coefficient, C_m C/4 reference, nose up positive</u>					
$\alpha = 1 \pm 1$	-.1577	-.6871	.0781	.6916	173.52
$\alpha = 2 \pm 2$	-.1836	-.8514	.2610	.8509	162.96
<u>Location of Upper Surface Shock, x/C</u>					
$\alpha = 1 \pm 1$.6572	1.395	-.803	1.610	-29.93
$\alpha = 2 \pm 2$.6961	1.069	-.701	1.278	-33.25

3.0 OUTER FIELD BOUNDARY CONDITIONS

In all of the previously reported calculations, References 1 to 4, and in the results described above, the computation field was a 9.6 chord square (approximately) centered at airfoil midchord. On the field perimeter, flow properties have been held to assigned values throughout the process of solving any particular unsteady flow problem. The distributions of flow properties on the boundary were obtained by adding perturbations due to a vortex and a doublet (at the airfoil) to the freestream conditions. The vortex strength was set at a value appropriate for the lift at a mean angle-of-attack.

The distances from the four boundaries and the signal propagation speeds are such that disturbances emitted at the airfoil should not return by reflection off the boundaries for about thirteen time units. Here a time unit is:

$$\text{Unit } t \equiv \text{chord/freestream sound speed}$$

The solutions for problems on sinusoidally oscillating airfoils all required more than 13 time units before an acceptably repeatable oscillatory response was obtained and, hence, all contain the influences of the approximations in perimeter boundary conditions. An attempt has been made to determine consequences of the arbitrary method used for assigning boundary conditions at the field perimeter.

The problems of concern in the present research involve lifting airfoils in subsonic unbounded freestreams. The pattern of disturbances (of velocity, pressure, etc.) from freestream conditions are caused by the airfoil; in the calculations these disturbances are generated by emitting pressure waves so that boundary conditions are satisfied at the surface. The wave fronts emitted from centers at the airfoil expand radially and are swept downstream. With the exception of a trailing vortex sheet (on unsteady problems) and an entropy wake (on problems with imbedded supersonic flow and shocks), the disturbances caused by the airfoil attenuate with distance from the airfoil. Thus, near the airfoil, a numerical solution done over a finite computation field may be hoped to be an adequate representation of the solution in an infinite stream whether the disturbances at the perimeter of the working field are set to their correct (but small) values, or some highly idealized approximate values, or even zero.

Application of approximate boundary conditions at the perimeter of the computation field still must be done with caution. Disturbances do not decay toward zero with distance from the airfoil in a uniform manner. For example, velocity perturbations will be stronger above and below the airfoil than ahead of the airfoil depending on the closeness of the freestream Mach number to unity. As a first approximation, the perturbations at large distances from the airfoil are sometimes regarded as representable by perturbations from vortex and doublet singularities of appropriate strengths located somewhere near the airfoil. This sort of approximation has been used in the computer program utilized in the present research. It should be recalled that the strengths of velocity perturbations due

to a doublet (roughly representing airfoil thickness effects) are inversely proportional to distance from the singularity squared. The velocity perturbations due to a bound vortex (representing airfoil lift effects) are inversely proportional to distance and in steady flow the circulation (line integral of velocity perturbations) along any contour surrounding the airfoil is supposed to a constant. Therefore, when obtaining a solution to a steady flow problem, the pattern of disturbances on the field perimeter is set so that the circulation agrees with the amount expected from the airfoil lift. This is analagous to the process of setting the potential on the outer perimeter to have the proper jump across the wake in a program based on the transonic potential equation.

In the computer program the Kutta condition is enforced and, therefore, the circulation level is set ultimately by application of finite difference approximations to derivatives of various functions in the vicinity of the trailing edge. In a steady flow problem, the setting of a new, different, circulation level at the outer perimeter will affect circulation on interior contours and affect the circulation achieved (and therefore the lift) at the airfoil by altering the balance of truncation errors in the approximations near the trailing edge. A direct test of this on a problem of steady Mach 0.72 flow over the 64A410 airfoil at 4 degrees angle-of-attack, but with outer perimeter circulation set to agree with lift at 2 degrees angle-of-attack, showed, for example,

$$d \Gamma (\text{airfoil}) / d \Gamma (\text{outer perimeter}) = 0.0775$$

Inasmuch as the lift is proportional to the circulation (Γ), the normal force and pitching moment at the airfoil can also be affected by an incorrect circulation level at the outer boundary of the computation field.

The effect on the airfoil circulation of the circulation maintained on the finite field perimeter causes difficulty when one considers calculating unsteady flow problems involving lift changes. If, say, there is a step change in angle-of-attack causing a step change in lift, a starting vortex is swept downstream from the trailing edge. Additional vorticity will continue to be shed as the starting vortex moves downstream. The circulation on the outer field perimeter will remain unchanged at first because the outer perimeter contains both the starting vortex and the (equal, but opposite sign) enhancement of the airfoil bound vortex. Ultimately the starting vortex will be convected to the downstream boundary of the computation field. If the "outer perimeter" were merely an interior contour in a (much larger) computation field, the starting vortex would continue being convected downstream, be removed from the interior of the "outer perimeter" and the circulation on the outer perimeter would jump to the value compatible with the enhanced bound vortex at the airfoil. The distribution of velocity perturbations on the "outer perimeter" would be peculiar at first along the downstream border because of close proximity to the receding starting vortex, but the velocity pattern would asymptotically approach the pattern associated with an airfoil in steady flow.

If, as in the present computer program, the "outer perimeter" is a real boundary of the computation field, and if we retain fixed conditions at the boundary, the starting vortex

will be unable to penetrate the boundary and will be dissipated by "numerical viscosity." The circulation will remain fixed at the outer boundary and this fixing will inhibit the buildup of lift at the airfoil to the final value which would have been achieved in an unrestricted field. Similar inhibition of lift changes can be envisioned if the airfoil executes some sinusoidal oscillation schedule.

For a first estimate of the effects on the oscillatory normal force and pitching moment of having held fixed conditions on the outer perimeter of the computation field, the oscillatory responses have been calculated from indicial responses by the use of convolution integrals, a method appropriate to linear systems. As described in References 2 and 4, the responses to step changes in α and $\dot{\alpha}$ were calculated for the case of the 64A410 at $\alpha = 2$ in Mach 0.72 flow. The responses were determined for 12 time units (unit $t = \text{chord}/\text{freestream sound speed}$) which is shorter than the time necessary for signals originating at the airfoil to have returned from the field perimeter by reflection. Twelve time units, however, is enough time for signals originating at the trailing edge to have made at least three circuits around the airfoil via a path forward along the lower surface and aft along the upper. The completion of the indicial response (Wagner) functions for $t > 12$ was then carried out in two manners:

- A. Asymptotic approach toward final values that might be realized in an unbounded stream (as deduced from proper steady-flow calculations at the final angle-of-attack).
- B. Asymptotic approach toward final values that would be attained in a steady flow calculation which maintained the outer perimeter circulation at the level prevailing before the step change.

The results for a number of reduced frequencies of sinusoidal pitching oscillations (mid-chord axis) of the 64A410 at 2° mean α in Mach 0.72 flow are shown in Figures 8 and 9. The results using Method B above (restricted computation field with fixed perimeter boundary conditions) have been presented earlier in Reference 4. The differences in the two results are small at reduced frequency 5.0, but are appreciable at reduced frequency 0.2. At reduced frequency 0.2 the predicted results of removing the constraints of the boundary conditions at the field perimeter are (principally) increases in the lag of the responses behind the motion. The lag increase expected is on the order of 4.5° for normal force and 9.8° for the pitching moment; the amplitude of the pitching moment response might be increased about 5% as well. Conversely, if the constraints of the perimeter boundary conditions were to be increased by (say) moving the perimeter closer to the airfoil, the oscillatory responses in normal force and pitching moment should be expected to change in phase toward the leading direction and probably the amplitude of the pitching moment response would be reduced.

For a second look at the probable effects of freezing conditions at the outer perimeter of the computation field, the calculations on the reduced frequency 0.2 pitching oscillatory

flow over the 64A410 at mean angle-of-attack of 1.0 degree in Mach 0.72 (described in the previous section) were repeated with different sizes for the computation field. The outer perimeter for the basic calculation was a square of 9.6 chords. The repeated calculations placed the outer perimeter on squares of 4.8 chords and 14.4 chords, respectively.

On the assumption that the strongest effect of freezing conditions on the outer computation perimeter is to reduce oscillatory components of a vortex character, one should expect that the amount of constraint depends inversely on the distance of the perimeter from the airfoil. Thus, one would expect that the calculation with boundary at 4.8 chords would have roughly two times as much boundary influence as the calculation with boundary at 9.6 chords; the expected factor for a boundary at 14.4 chords is 2/3.

Figures 10 to 13 show selected response characteristics with the outer perimeter set at three different distances from the airfoil. Moving the boundary closer to the airfoil (4.8 chord square) does seem to shift the peaks in pitching moment and normal force responses to occur earlier in the cycle and to somewhat reduce the amplitude of the pitching moment response. The changes due to moving the boundary out to a 14.4 chord square are not very dramatic. Moving the boundary in to 4.8 chords seems to inhibit development of the circulatory flow as a whole with reductions in the time-averaged mean values of normal force and pitching moment. Table III shows the (normalized) oscillatory responses for normal force and pitching moment calculated with the three different outer field sizes.

Table III

Effect of Outer Field Size on Calculated Oscillatory Response

64A410 Mach 0.72 $\alpha = 1 \pm 1^\circ$ $k = 0.2$
Mid-chord Oscillation Axis

$$\alpha(t) = \alpha_0 + \tilde{\alpha} \sin(\omega t)$$

First Harmonic of Response Listed

$$f(t) = B_0 + S_1 \sin(\omega t) + C_1 \cos(\omega t)$$

$$= B_0 + A_1 \sin(\omega t + \phi_1)$$

Responses normalized, per radian of oscillation amplitude

Function, Field Size	B_0	S_1	C_1	A_1	ϕ_1
Normal Force Coefficient, C_N					
4.8 Chord Square	.8223	7.038	-2.108	7.347	-16.67°
9.6 Chord Square	.8445	6.976	-2.884	7.549	-22.46°
14.4 Chord Square	.8474	6.834	-2.998	7.462	-23.68°
Pitching Moment Coefficient, C_m (C/4), Nose Up Is Positive					
4.8 Chord Square	-.1453	-.6404	.0199	.6407	178.22°
9.6 Chord Square	-.1577	-.6871	.0781	.6916	173.52°
14.4 Chord Square	-.1601	-.7103	.1075	.7184	171.39°

The effects of different degrees of boundary constraint predicted from the super-position of indicial responses are qualitatively confirmed by the results shown in Table III. The further out the perimeter boundary is placed, the more phase lag in oscillatory normal force and pitching moment responses and the more amplitude in the pitching moment response.

To possibly assist in judging the feasibility of applying a more sophisticated outer perimeter boundary condition in working on problems involving oscillatory flow, an examination has been made of the pressures in the outer field. For the 64A410 at Mach 0.72, $\alpha = 1 \pm 1^\circ$, with a mid-chord oscillation axis and reduced frequency 0.2, the pressures at nodes in the outer field distributed along a circle (of radius 3.6 chords) circumscribed about the airfoil mid-chord have been examined. These results are from the basic case with 9.6 chord square outer field boundary.

The time-averaged mean pressure coefficient has a plausible distribution, Figure 14, with peak negative pressures above the lifting airfoil and peak positive pressures below the airfoil.

The magnitudes of the first harmonics of the oscillatory pressures show some tendency to be largest near loci having large (absolute) steady pressure perturbations, $|\overline{C_p}|$. The phases of the oscillatory components are comparatively uniform in the half circle below the airfoil, but have more lag ahead than aft. The peak positive pressure excursions occur from 15 to 55 degrees after peak angle of attack. In the upper half circle, the phase angles cover a considerable range; the lag in peak negative C_p after maximum angle of attack is about 50 degrees directly above the airfoil.

The pressures at this (3.6 chord) radius from a lifting airfoil lack the y-antisymmetry and the simplicity of form (that is, ϕ_{ff}^I is evidently not independent of ϕ_{ff}^0) of the farfield solution described in Reference 5.

4.0 EFFECT OF TRANSFER OF AIRFOIL BOUNDARY CONDITIONS TO THE MEAN POSITION OF THE OSCILLATING AIRFOIL

In all calculations of flows over oscillating airfoils performed to date on the present contract, the airfoil surface boundary conditions have been satisfied at discrete fixed locations in the physical plane arrayed along a contour which would coincide with the airfoil if the airfoil were in its time averaged location. The objective here is to determine the consequences of the approximation of satisfying the boundary conditions at fixed (mean) loci rather than at points along the moving airfoil.

The computer program is designed to obtain numerical approximations to solutions for the unsteady Euler equations in conservative form:

$$\partial(\rho)/\partial t = -\partial(\rho u)/\partial x - \partial(\rho v)/\partial y \quad (1)$$

$$\partial(\rho u)/\partial t = -\partial(\rho u^2 + p)/\partial x - \partial(\rho uv)/\partial y \quad (2)$$

$$\partial(\rho v)/\partial t = -\partial(\rho uv)/\partial x - \partial(\rho v^2 + p)/\partial y \quad (3)$$

$$\partial(E)/\partial t = -\partial[u(E+p)]/\partial x - \partial[v(E+p)]/\partial y \quad (4)$$

Here, the usual meanings for fluid mechanics problems apply:

ρ = fluid density

p = pressure

u, v = Cartesian fluid velocity components

x, y = Cartesian (space-fixed) coordinates

t = time

γ = adiabatic index

$$E = p/(\gamma - 1) + (\rho/2)(u^2 + v^2) \quad (5)$$

= total energy per unit volume

The coupled system of equations, (1) - (4) has the form:

$$\partial W/\partial t = -\partial F/\partial x - \partial G/\partial y \quad (6)$$

where W , F and G are four element vectors whose elements may be discerned by inspection of (1) - (4).

In the computer program the system represented by (6) is solved approximately by setting up arrays of about 6000 points in the X-Y plane at which the 4 components of the dependent variable W are defined; the elements of F and G are non-linear functions of the elements of W. The partial derivatives on the right hand side are approximated by finite-differences between values of F or G at suitably adjoining mesh nodes near the point being worked on and the values of W are integrated, approximately, in time using discrete time steps. In the existing computer program, airfoil boundary conditions are maintained at (on the order of) 100 of the mesh nodes distributed along a contour which would coincide with the airfoil if the airfoil were in its mean position.

First, the manner in which airfoil boundary conditions have been applied in the calculations done to date will be reviewed. Referring to Figure 15, assume a system of coordinates X, Y, affixed along and normal to the airfoil chord.

The airfoil shape, considered rigid here, may be given, parametrically, as functions $X_a(s)$, $Y_a(s)$; that is the X_a , Y_a pairs of points along the airfoil contour are functions of a parameter, s, which could be, say, distance from the trailing edge as the airfoil is traced in a clockwise manner. The inclination of the clockwise tangent to the surface is:

$$\tan \theta = (dY_a/ds) / (dX_a/ds) \quad (7)$$

and the outwardly directed surface normal would be in the direction $\theta + \pi/2$.

Now, assume that the airfoil executes some oscillatory motion with respect to a Cartesian reference system, x, y. In particular we might wish to study sinusoidal pitching oscillations about an axis on the airfoil chordline a certain distance X_c aft of the nose. Referring to Figure 15 the pitch angle, called β here, may be a function of time of the form:

$$\beta(t) = A \sin(\omega t) \quad (8)$$

and its time derivative is:

$$\dot{\beta}(t) = \omega A \cos(\omega t) \quad (9)$$

Instantaneously, the location in the x, y system of a particular node point m affixed to the moving airfoil at X_m , Y_m would be:

$$\begin{aligned} x_m &= x_c + (X_m - X_c) \cos \beta + Y_m \sin \beta \\ y_m &= -(X_m - X_c) \sin \beta + Y_m \cos \beta \end{aligned} \quad (10)$$

Of course, since β is a sinusoidal function of time, the location of point "m" has Cartesian velocity components

$$\begin{aligned}\dot{x}_m &= \dot{\beta} [-(X_m - X_c) \sin \beta + Y_m \cos \beta] \\ \dot{y}_m &= \dot{\beta} [-(X_m - X_c) \cos \beta - Y_m \sin \beta]\end{aligned}\tag{11}$$

The instantaneous direction of the clockwise surface tangent through X_m, Y_m is

$$\theta_m = \Theta_m - \beta\tag{12}$$

and the direction of the outward normal is

$$\theta_m + \pi/2.$$

The proper, inviscid, boundary condition on the flow at a node X_m, Y_m affixed to the rigid, but moving, airfoil contour is that the flow velocity relative to the moving node "m" must have zero component in the instantaneous direction of the local surface normal. Thus, in the computer program, when boundary conditions are to be satisfied at a particular mesh node m at time t:

- a. the airfoil pitch angle β and pitching angular velocity are calculated for time t using Eqs. (8) and (9) (these are independent of the particular node, m).
- b. the inclination angles of the local surface tangent and normal are calculated from Eq. (12).
- c. the Cartesian fluid velocity is resolved into components along and normal to the instantaneous surface tangent:

$$\begin{aligned}v_{\text{tan}} &= u \cos \theta_m + v \sin \theta_m \\ v_{\text{nor}} &= -u \sin \theta_m + v \cos \theta_m\end{aligned}\tag{13}$$

- d. the fluid velocity in the direction of the local surface normal is adjusted to match the component of velocity of node m in that direction; this adjustment causes changes in the density and pressure but no change in the tangential velocity.

$$\begin{aligned}\tilde{v}_{\text{tan}} &= v_{\text{tan}} \\ \tilde{v}_{\text{nor}} &= -\dot{x}_m \sin \theta_m + \dot{y}_m \cos \theta_m\end{aligned}\tag{14}$$

e. the new fluid velocity is resolved back to Cartesian components.

$$\begin{aligned}\tilde{u} &= \tilde{v}_{\tan} \cos \theta_m - \tilde{v}_{\text{nor}} \sin \theta_m \\ \tilde{v} &= \tilde{v}_{\tan} \sin \theta_m + \tilde{v}_{\text{nor}} \cos \theta_m\end{aligned}\tag{15}$$

f. the adjusted density, pressure, and Cartesian velocity components are used to recalculate the primary dependent variables; that is, the four elements of the vector W .

There are no severe approximations in the procedure for satisfying airfoil boundary conditions described above. The main approximation in the computer program used to date is that this procedure has been applied at nodes fixed in the Cartesian (x, y) space rather than at nodes affixed to the moving airfoil. That is, in Equation (10) the approximation has been made that the motion is small and that it would be acceptable to set

$$\begin{aligned}x_m &\doteq X_m \\ y_m &\doteq Y_m\end{aligned}\tag{16}$$

Actually, for a problem involving an airfoil pitching about midchord with 2 degree amplitude, the y excursions of the nose and the trailing edge would be ± 0.017 chords so airfoil boundary conditions would be satisfied at 0.017 chords from the correct location. More pertinent, since this is the case actually worked on to evaluate the errors, is the case of an airfoil executing plunging oscillations of 0.0436 chord amplitude at reduced frequency 0.4. This combination of excursion amplitude and reduced frequency is such that the maximum plunging velocity (when divided by free stream velocity) is equivalent to one degree induced angle of attack.

To study the effect of the above approximation, the program has been temporarily revised to allow computations in a rigid grid system attached to the rigid (but moving) airfoil. The approach used follows that outlined in a note by Viviand, Ref. 6.

Following Viviand, assume we are using the gas dynamics equations in 2 space dimensions in conservative form and rewrite Eq. (6) as:

$$\partial W / \partial t + \partial F_i / \partial x_i = 0. \quad (i = 1, 2)\tag{17}$$

W and F_i are each 4 component vectors (in our case) and the convention of repeated indexes indicates summation.

Define a new system of coordinates which has relations to the old which can be functions of time:

$$\begin{aligned} X_i &= X_i(x_1, x_2, t) \\ \tau &= t \end{aligned} \quad (18)$$

and, by application of chain rules for differentiation, the gas dynamics equations come out in non-conservative form:

$$\frac{\partial W}{\partial \tau} + \frac{\partial X_j}{\partial t} \frac{\partial W}{\partial X_j} + \frac{\partial X_j}{\partial x_i} \frac{\partial F_i}{\partial X_j} = 0 \quad (19)$$

Using this form has disadvantages in complication of the treatment of discontinuities such as shocks. The equations can be brought back to conservative form in the new coordinates by use of the Jacobian of the transformation of coordinates:

$$D = \frac{\partial(X_1, X_2)}{\partial(x_1, x_2)} \quad \text{and} \quad \frac{1}{D} = \frac{\partial(x_1, x_2)}{\partial(X_1, X_2)} \quad (20)$$

Viviand shows that the proper conservation form of the new coordinates is:

$$\frac{\partial}{\partial \tau} \left(\frac{W}{D} \right) + \frac{\partial}{\partial X_j} \left(\frac{W}{D} \frac{\partial X_j}{\partial t} + \frac{\partial X_j}{\partial x_i} \frac{F_i}{D} \right) \quad (21)$$

and that the jump conditions at discontinuities for this system are identical to jump conditions for the original system. Therefore, shocks treated by a shock-capturing difference scheme should appear with the same properties as they would have in the original system, Eq. (17).

As a specific example for evaluating the errors attendant with satisfying boundary conditions at a fixed location rather than on the moving airfoil, the Mach 0.8 flow over the NACA 64A010 airfoil at zero angle of attack has been chosen. The airfoil is oscillating sinusoidally in a plunging motion of amplitude 0.0436 chords at a reduced frequency 0.4 (based on chord). This example was chosen, as a matter of expediency, because:

- a. it is a worthwhile example since this airfoil is to be tested at this Mach number in experiments planned at NASA Ames Research Center.
- b. the Jacobian of the coordinate transformation takes a particularly simple form which could be incorporated into the existing computer program with a minimum of modifications.

- c. choosing an example with zero average lift and no angular excursions avoids conceptual complications concerning the (also troublesome) outer field boundary condition.

Therefore, consider an airfoil-fixed coordinate system (X, Y) with X aft along the chordline from the airfoil nose and Y upward and an inertial Cartesian system (x, y). The relation between the two sets for the plunging motion described above is:

$$\begin{aligned}x &= X \\y &= Y - A \sin (\omega \tau) \\t &= \tau\end{aligned}\tag{22}$$

where:

$$A = 0.0436 \text{ chord and } \omega = kU_{\infty}/\text{chord.}$$

It may be noted that the plunging velocity of the airfoil is

$$\dot{y}_a = -A \omega \cos (\omega \tau)\tag{23}$$

which has a peak value of $0.01745 U_{\infty}$ so the "induced" angle of attack is 1.0 degree.

The inverse Jacobian of the transformation, Eq. (20) is:

$$\begin{bmatrix} 1 & 0 \\ 0 & 1 \end{bmatrix} = 1$$

Therefore, the proper conservation form for the moving system attached to the plunging airfoil (X, Y, τ) is: (after putting it into the form analagous to Eq. (6))

$$\begin{aligned}\frac{\partial W}{\partial \tau} &= -\frac{\partial F}{\partial X} - \frac{\partial}{\partial Y} \left(G + W \frac{\partial Y}{\partial t} \right) \\ &= -\frac{\partial F}{\partial X} - \frac{\partial}{\partial Y} \left(G + WA \omega \cos (\omega \tau) \right) \\ &= -\frac{\partial F}{\partial X} - \frac{\partial}{\partial Y} \left(G - \dot{y}_a W \right)\end{aligned}\tag{24}$$

Thus, in the computer program, it is only necessary to replace G by $G - \dot{y}_a W$ where \dot{y}_a is a function of time only.

Comparisons between the results of these calculations with the boundary conditions satisfied along a fixed (mean) contour in space and satisfied on the moving airfoil are shown in Figures 16 through 21. The abscissa in a number of these figures is defined

$$\phi = \omega\tau \text{ in degrees}$$

where $\omega\tau$ is the argument for the sinusoidal plunging motion, Eq. (22). Where $\phi = 0$, the airfoil has maximum downward velocity.

The normal force coefficient, pitching moment coefficient about the quarter chord and the location of the lower surface shock are shown in Figures 16 - 18 and summarized in Table IV.

The magnitudes of the C_N excursions agree reasonably well. The peak C_N for fixed B.C. nodes occurs about 5° later in the cycle (40° after maximum downward plunge velocity rather than 35° after maximum plunge speed for the calculation with moving B.C. nodes). The pitching moment excursions for the two calculations differ quite dramatically from one another; the amplitude when B.C. nodes are fixed is .01861, whereas it is .01051 when the B.C. nodes are on the moving airfoil. Similarly, the shock motion amplitude is greater by a factor of .05544/.04518 when the B.C. nodes are fixed rather than moving. Expressed as vectors, the discrepancies between the results of the 2 calculations have magnitudes which are appreciable fractions of the magnitude of the basic response vectors, 0.083 for C_N , 0.84 for C_m , and 0.29 for the shock movement.

Loading-style chordwise pressure distributions at 30 degree phase intervals for the calculations with boundary conditions satisfied at nodes on the moving airfoil are shown in Figure 19. Only half a cycle is covered formally; since the airfoil and the motion are symmetric, the second half of the cycle can be examined by interchanging the labels "upper surface" and "lower surface" in this figure. It may be noted that there is relatively little loading on the aft part of the airfoil over most of the cycle and that the lower surface shock becomes quite weak in the vicinity of $\phi = 90^\circ$.

Traces showing the lower surface pressure fluctuations at two stations ahead, one near the shock, and two stations aft of the shock are shown in Figure 20. For the stations which are not traversed by the shock the pressure traces may be seen to be reasonably sinusoidal. Ahead of the shock (see $X/C = 0.14$ and $X/C = 0.30$) the pressure excursions are noticeably smaller when the boundary conditions are satisfied at fixed nodes than when they are satisfied at nodes on the moving airfoil. Aft of the shock (see $X/C = 0.66$ and $X/C = 0.82$) the reverse is true. If the

Table IV

Comparison of Results
 From Calculations with Boundary Conditions Satisfied
 At Nodes on the Moving Airfoil or at Fixed Nodes
 64A010 Mach 0.80 $\alpha = 0$ $k = 0.4$
 Plunging Velocity = $-0.01745U_\infty \cos(\omega t)$
 Single Harmonic Representation of Response

$$f(t) = B_0 + S_1 \sin(\omega t) + C_1 \cos(\omega t)$$

$$= B_0 + A_1 \sin(\omega t + \phi_1)$$

Function	B_0	S_1	C_1	A_1	ϕ_1
<u>Normal Force Coefficient, C_N</u>					
Fixed nodes	-.00051	.06719	.08145	.10559	50.48
Moving nodes	-.00034	.06011	.08664	.10546	55.25
Fixed result - Moving result	-.00017	.00708	-.00519	.00878	-36.24
<u>Pitching Moment Coefficient, C_m C/4 reference, nose up positive</u>					
Fixed nodes	.00000	-.00502	-.01792	.01861	-105.64
Moving nodes	.00002	-.00004	-.01051	.01051	-90.22
Fixed result - Moving result	-.00002	-.00498	-.00741	.00893	-123.90
<u>Location of Lower Surface Shock, x/C</u>					
Fixed nodes	.52949	-.04746	-.02866	.05544	-148.87
Moving nodes	.52738	-.03426	-.02945	.04518	-139.32
Fixed result - Moving result	.00211	-.01320	.00079	.01322	176.57

point of view is taken, that satisfying boundary conditions at fixed nodes merely deletes terms from the differential equations (compare Eq. 24 to Eq. 6) and that the effects might be localized in space and time, one ought to expect the pressures from the two solutions to agree when the plunging velocities are zero; that is, at $\phi = 90^\circ$ and $\phi = 270^\circ$. Inspection of the traces in Figure 20 shows the above reasoning to be approximately valid.

That the differences in the two oscillatory solutions are significant is further illustrated in Figure 21. The calculated pressure oscillations at a number of locations on the lower surface of the airfoil were fitted with single harmonics of the form:

$$p(\phi) = B_0 + A_1 \sin(\phi + \phi_1)$$

by at least squares procedure.

The mean pressure distributions differ noticeably only in the region traversed by the moving shock. The amplitudes and phase angles are shown also in Figure 21.

In summary, satisfying the airfoil boundary condition at fixed nodes rather than at nodes on the moving airfoil had the following effects (for the particular plunging problem studied):

- a. decreased the pressure fluctuations on the forward part of the airfoil.
- b. increased the pressure fluctuations on the aft part of the airfoil
- c. increased the excursions in shock location.

The resultant effect on the normal force fluctuations was to shift the phase angle at which the normal force reached its maximum to about 5 degrees later in the cycle. The pitching moment fluctuations were increased to about 1.8 of the value when boundary conditions were satisfied at nodes on the moving airfoil and peak values of pitching moment came about 15 degrees later in the cycle.

5.0 CONCLUDING REMARKS

A primary objective of the research was the calculation of some examples of unsteady flows over airfoils by a straightforward method. The results were intended to serve as test solutions to which results from simpler, more approximate, methods could be compared.

In the computer program used in this research study, features were included which would not have been used if the program had been designed for routine production use. The usage of four coupled equations is unnecessary for most of the flowfield; the unsteady potential equation probably would have done equally well for most problems and for most parts of the field on severe problems. The complexity of the Euler equations is needed only for tracking the motion of the shock with the shock capturing scheme and for detailing the flow over the aft part of the airfoil behind a strong shock. The bulk of the computation time is expended for detailing the flow over the nose and the tracking of the shock. The flow over the nose could be handled better by use of the potential equation and an implicit scheme which would permit advancing the solution with fewer passes through the field. Actually, many of the main features of unsteady flow can be reproduced using perturbation potential programs with boundary conditions satisfied along the chordline; these programs treat the flow around the airfoil nose in an extremely roughshod manner.

The examples turned out, References 1 through 4, seem not to have been used much for checking other methods, possibly because they were too severe and at too high a reduced frequency. In Reference 7 the amplitudes of the pressure excursions for 64A410 pitching at $k = 0.2$ were compared to results presented in Reference 2. Unfortunately, no phase information was compared. That References 1 through 4 show the pressure changes on the upper surface of the airfoil aft of the shock are "out of phase" with those ahead of the shock in both steady flow angle of attack changes and in oscillatory flow at $K = 0.2$ was not commented upon in Reference 7. Integrated pressures were used to obtain the forces and moment about the nose of the airfoil; these were compared to the results in Reference 2. Comparing moments about the nose rather than the quarter chord tends to obscure the rather severe differences between the two solutions. The additional example of flow over the 64A410 oscillating about $\alpha = 1^\circ$ presented here, being less severe, may find more usage as a test problem.

The investigations reported here show that there are appreciable effects of approximations in satisfying boundary conditions at the airfoil surface and on the outer field perimeter.

The fixing of the outer perimeter flow conditions appears (Figure 9) to cause phase shifts in the pitching moment, at $k = 0.2$, of (on the order of) 10 degrees). It is not certain that these shifts could be eliminated by use of a stretched outer coordinate

mesh extending to infinity because the signals of concern may be severely attenuated in the coarsening outer mesh and because the distance coordinates may formally be removed toward infinity but the airfoil remains a finite number of grid lines (and computation steps) from the perimeter boundary condition in any practical numerical solution. Patching to a "far field" solution has the hazard that the outer solution may be unsuitable for the problem being worked on.

Caution probably should be exercised in usage of the results obtained here on the effects of freezing flow properties on the outer perimeter of the computation field. First, the results may be dependent on the details of the specific method and specific computer program used in evaluating the effects. Second, the hints are present in Figures 8 and 9 that the effects of the constraint are different at different reduced frequencies. It may be noted that the vector differences between the "bounded" and "unbounded" predictions (Figures 8 and 9) change direction as the reduced frequency is varied. Presumably, this is explainable by there being a rather definite lag time for the most influential signals to propagate from the airfoil to the field perimeter and return. The "mishandling" of the signals at the perimeter can return influence to the airfoil and either tend to reinforce or to cancel the cause of the original signals depending on phasing (which is dependent on reduced frequency).

A calculation satisfying airfoil boundary conditions on nodes fixed at the mean location of the oscillating airfoil was shown to have rather remarkable differences from the test solution with boundary conditions satisfied on the moving airfoil. The effects appear to be due to straightforward additional terms in the differential equations whose magnitudes depend on gradients of the primary dependent variables and the airfoil plunging velocity. In the example selected as a test problem the maximum plunging velocity was 0.01745 of the free stream velocity. Presumably, those problems worked earlier having plunging velocities of a similar magnitude could change upon recalculation by amounts approaching what was found here. Two of the three oscillatory problems on the 64A410 reported in References 1 through 4 have plunging velocities of $0.01745 U_\infty$ at the nose and trailing edge of the airfoil; namely the $k = 1.0$, $\alpha = 2 \pm 2^\circ$ case and the $k = 5.0$, $\alpha = 2 \pm 0.4^\circ$ case.

Inasmuch as the terms added to the differential equations when the problem is transformed to satisfy boundary conditions at nodes on the moving airfoil depend linearly on the airfoil velocities due to oscillation (compare Eqs. 6 and 24), their effect might become negligible if the amplitude of and velocities caused by the oscillations were reduced toward zero. The amplitudes of the response functions would tend toward zero also, so the relative orders of magnitude of the various terms should be studied. For thin airfoils with small gradients in the primary variables (W) in the vicinity of the airfoil, the extra terms should become negligible as the oscillation-caused

velocities approach zero. Thus, if the results of calculations already performed are normalized (by dividing response functions by the amplitudes of the motions executed) the normalized results should (ostensibly) be applicable to problems with vanishingly small oscillation amplitude. Of course, if one is attempting to calculate the flow over an airfoil oscillating with a definite amplitude (for example, to compare with an experiment in which the oscillations have finite amplitude) one ought to use care in the calculations to include the proper terms.

The effects of wall interference should be considered if the calculations are to be compared with data obtained in wind tunnels. Initial efforts to assess possible wind tunnel wall effects are reported by Traci, et al, in Reference 7.

Ultimately, if the calculations are to be of use in prediction of behavior to be expected on airfoils oscillating in real airstreams, the strong viscous effects occurring in transonic flows must be accounted for. In particular, the weakening of the pressure rise at the shock because of interaction with the boundary layer must be considered, and the lessening of the lift because of boundary layer buildup or separation at the trailing edge must be taken into account.

6.0 REFERENCES

1. Magnus, R. and Yoshihara, H. "Finite Difference Calculations of the NACA 64A410 Airfoil Oscillating Sinusoidally in Pitch at $M = 0.72$," General Dynamics Convair, CASD-NSC-74-004, 1 August 1974.
2. Magnus, R. J. and Yoshihara, H. "Calculations of Transonic Flow Over an Oscillating Airfoil," AIAA Paper 75-98, 13th Aerospace Sciences Meeting, Pasadena, California, January 20-22, 1975.
3. Ballhaus, W. F., Magnus, R., and Yoshihara, H. "Some Examples of Unsteady Transonic Flows Over Airfoils," Symposium on Unsteady Aerodynamics, University of Arizona, Tuscon, March 18-20, 1975.
4. Magnus, R. and Yoshihara, H. "Unsteady Transonic Flows Over an Airfoil," AIAA Journal, Vol. 13, No. 12, December 1975, pp. 1622-1628.
5. Traci, R. M., Albano, E. D., Farr, J. L. Jr., and Cheng, H. K. "Small Disturbance Transonic Flows About Oscillating Airfoils," Air Force AFFDL-TR-74-37, June 1974.
6. Viviani, Henri, "Formes Conservatives Des Équations De La Dynamique Des Gaz," La Recherche Aérospatiale, Ann. 1974, No. 1, January - February, pp. 65-68.
7. Traci, R. M., Albano, E. D. and Farr, J. L. Jr., "Small Disturbance Transonic Flows About Oscillating Airfoils and Planar Wings," Air Force AFFDL-TR-75-100, August 1975.

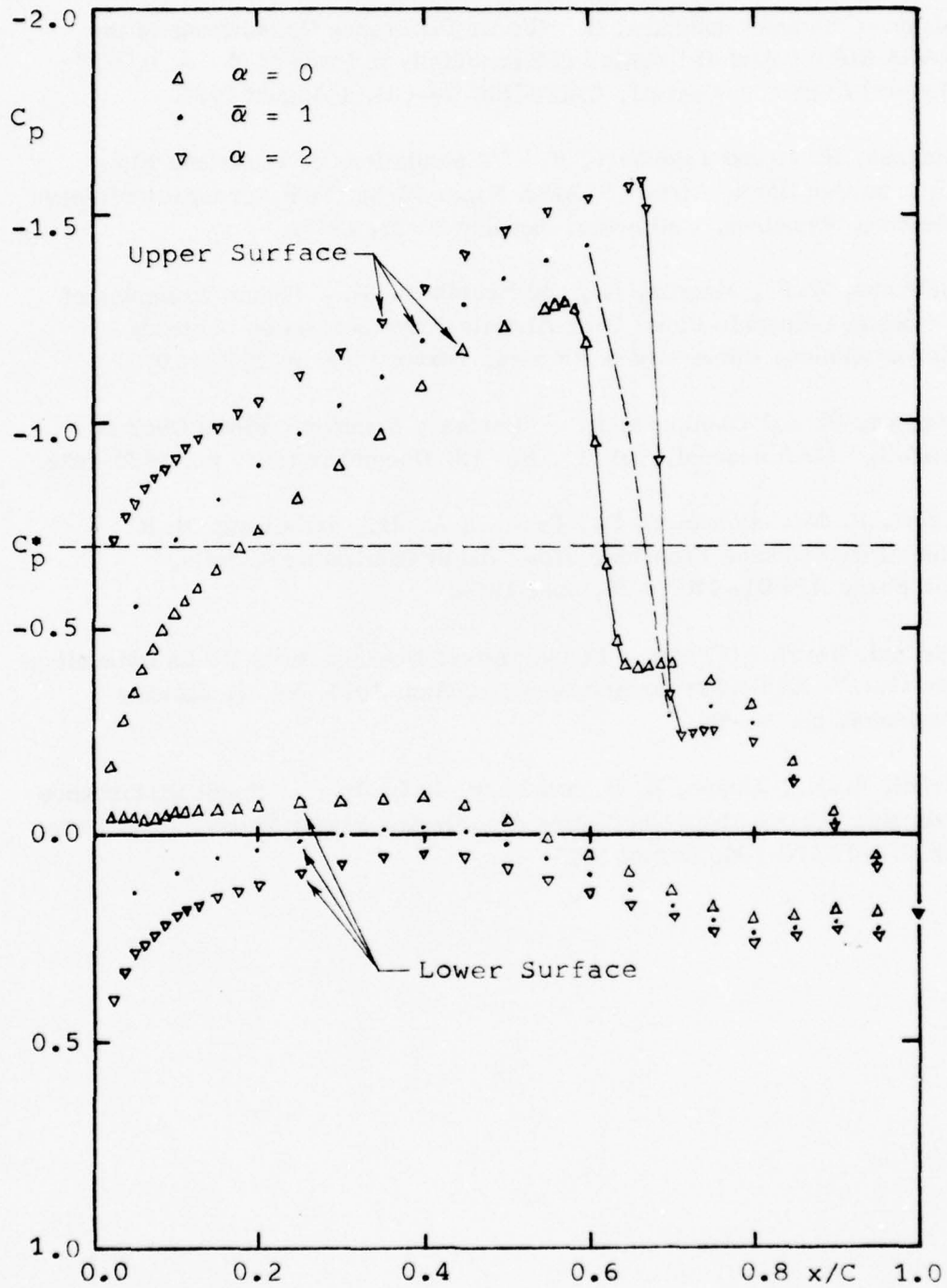


Figure 1. Pressure distributions on NACA 64A410 in Mach 0.72 flow; steady flow at $\alpha = 0, 2$ and mean value in oscillation about $\alpha = 1$.

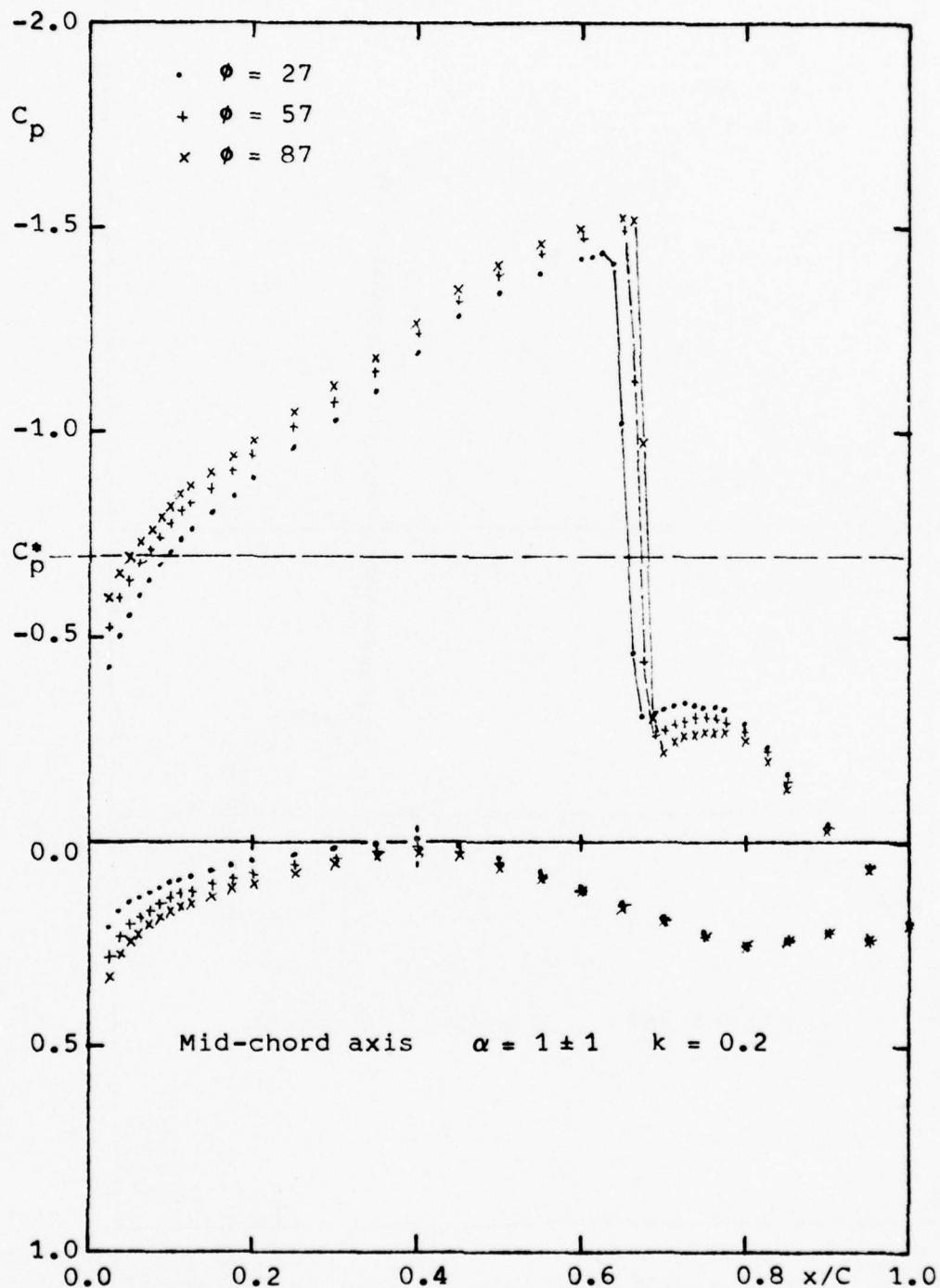


Figure 2. Pressure distributions on NACA 64A410 oscillating in Mach 0.72 flow. (a) $\phi = 27, 57, 87$.

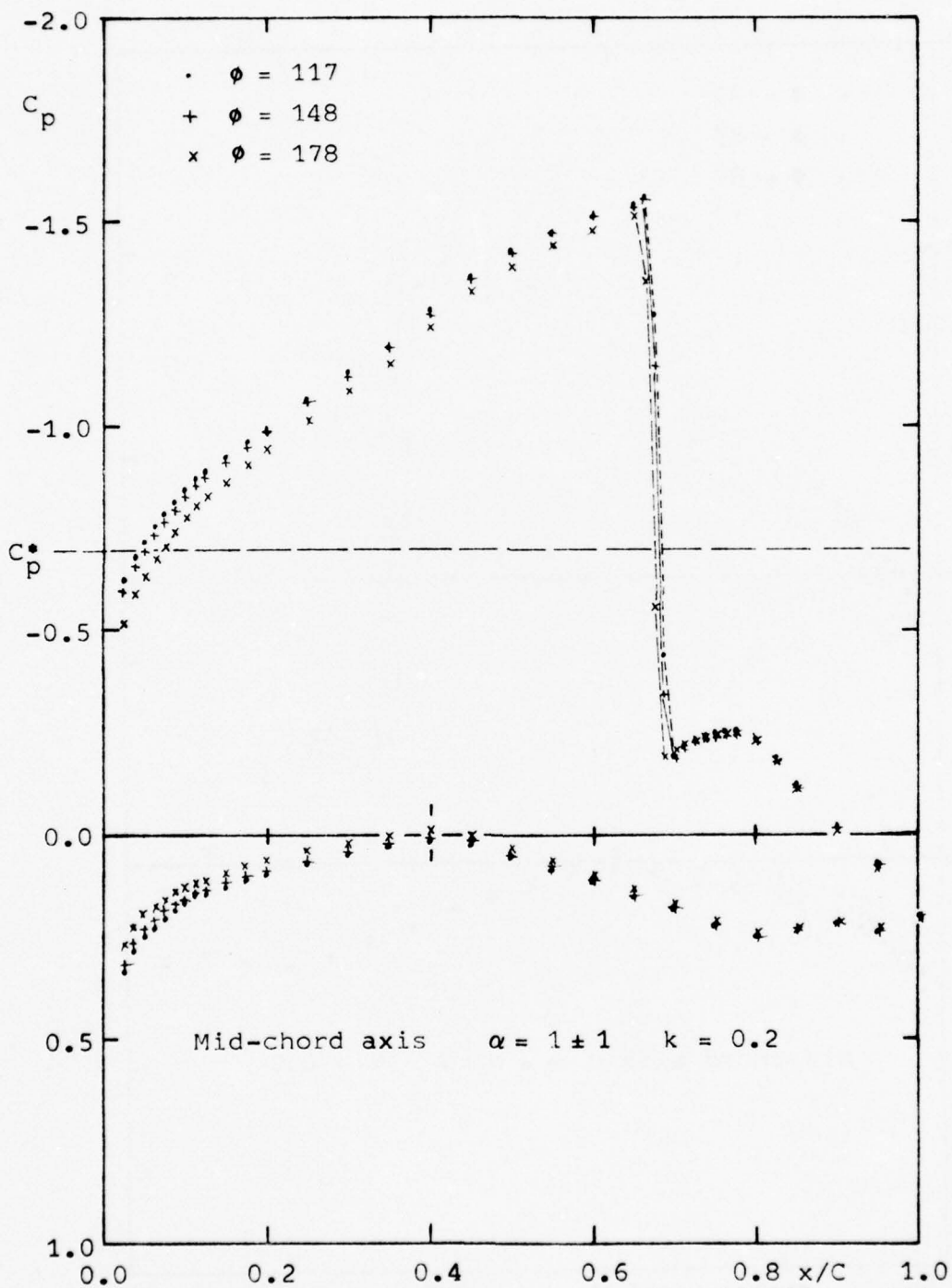


Figure 2. Pressure distributions on NACA 64A410 oscillating in Mach 0.72 flow. (b) $\phi = 117, 148, 178$.

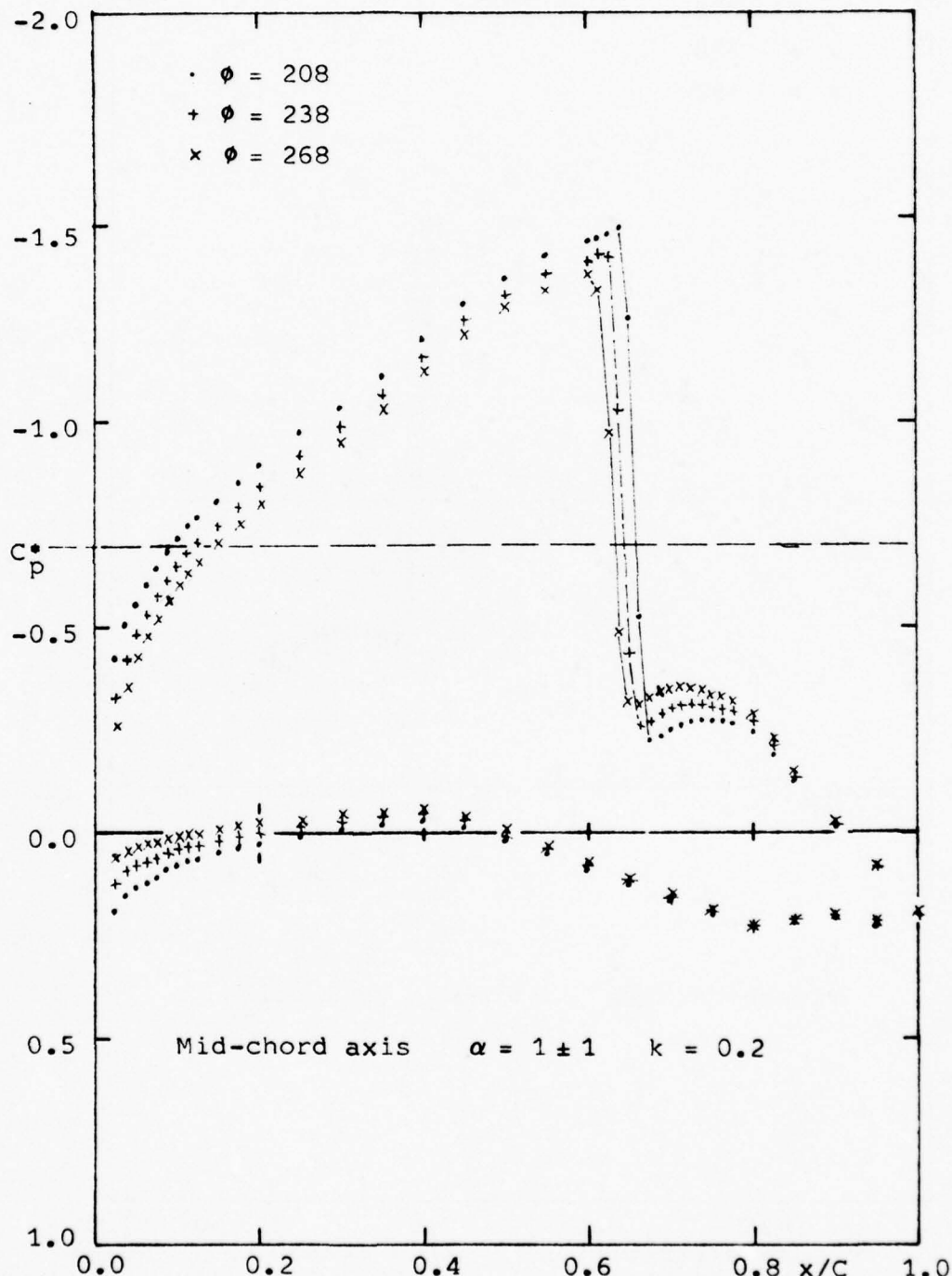


Figure 2. Pressure distributions on NACA 64A410 oscillating in Mach 0.72 flow. (c) $\phi = 208, 238, 268$.

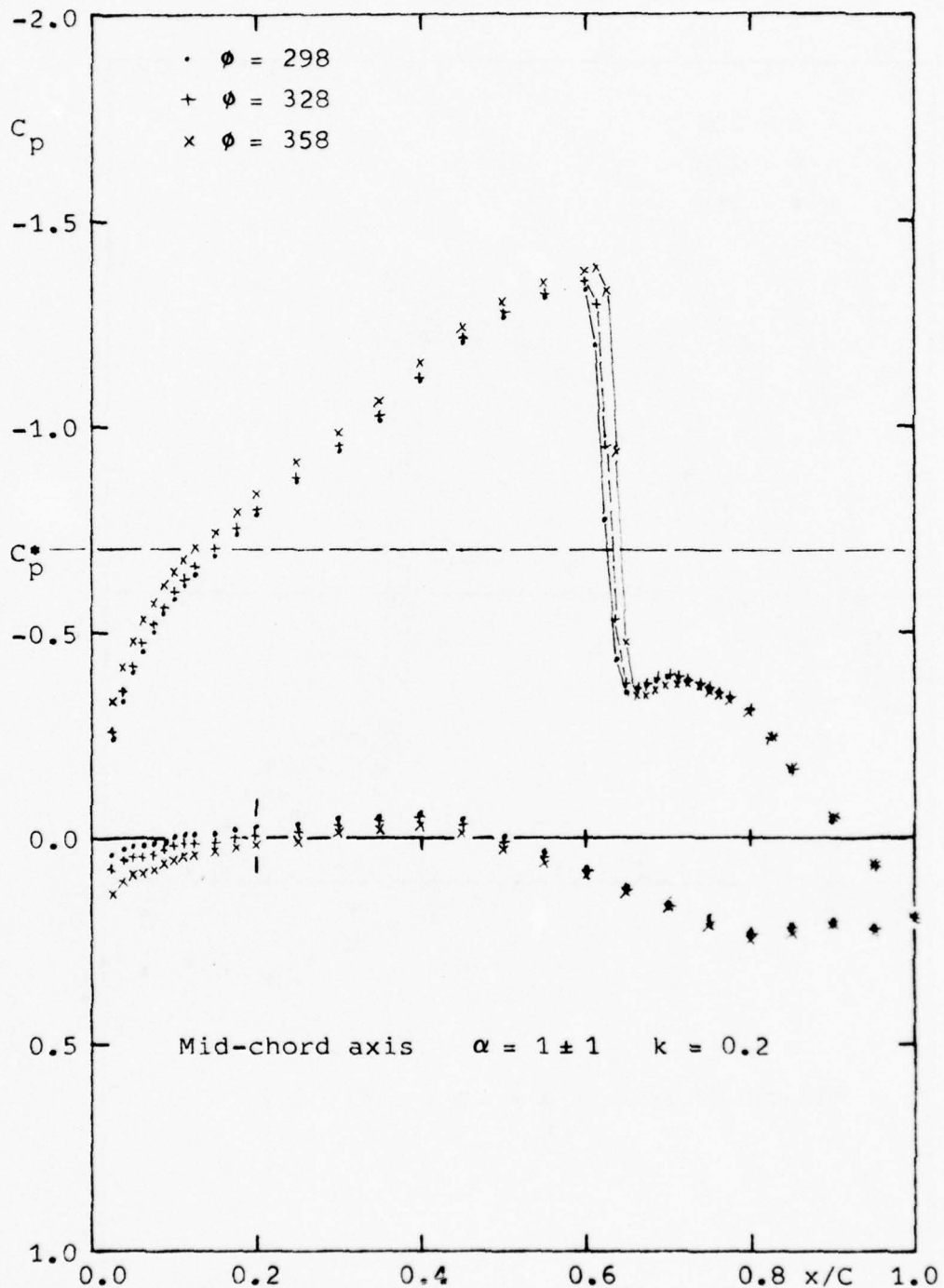


Figure 2. Pressure distributions on NACA 64A410 oscillating in Mach 0.72 flow. (d) $\phi = 298, 328, 358$.

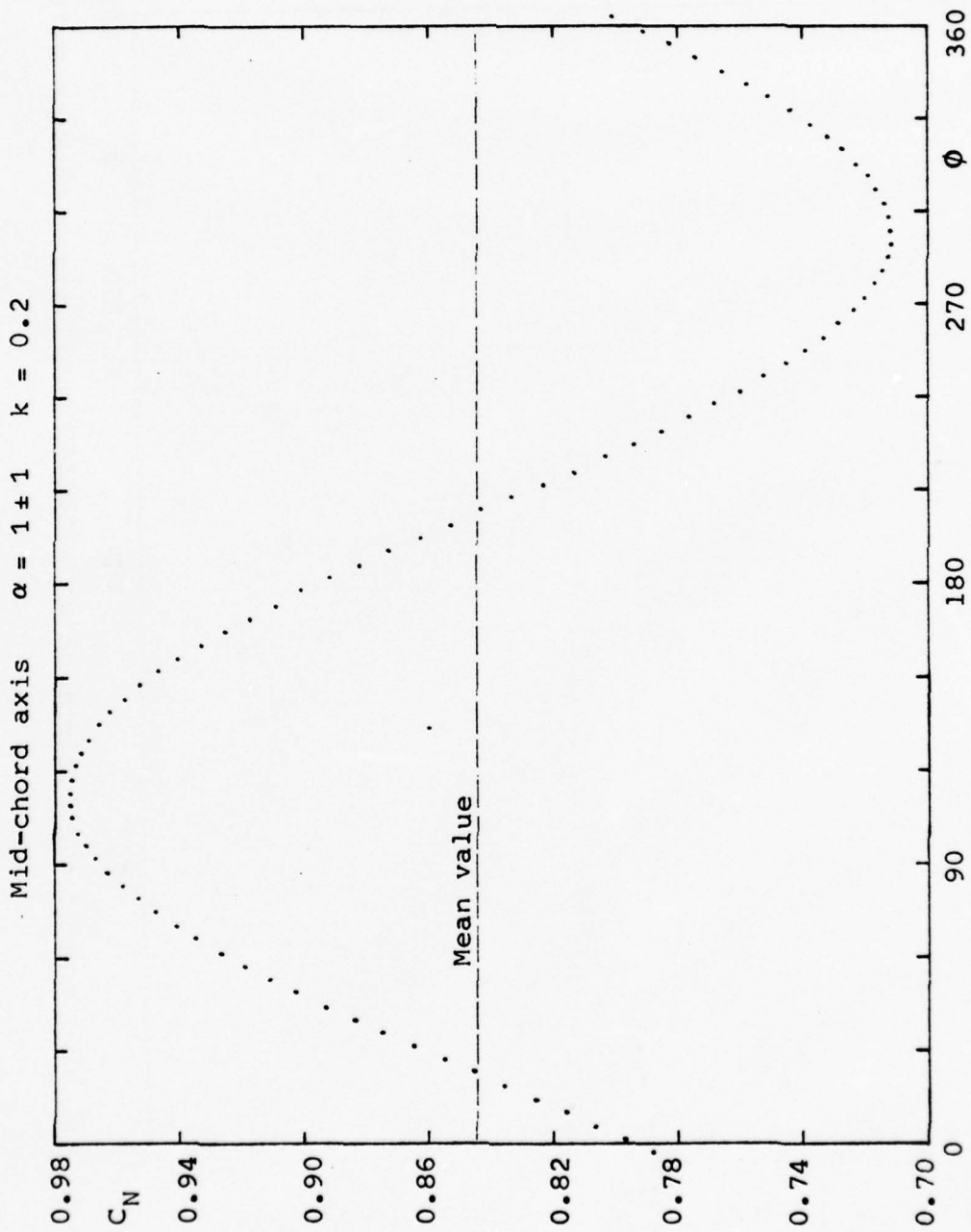


Figure 3. Normal force coefficient on NACA 64A410 oscillating in Mach 0.72 flow.

Mid-chord axis $\alpha = 1 \pm 1$ $k = 0.2$
C/4 reference, nose up moment positive

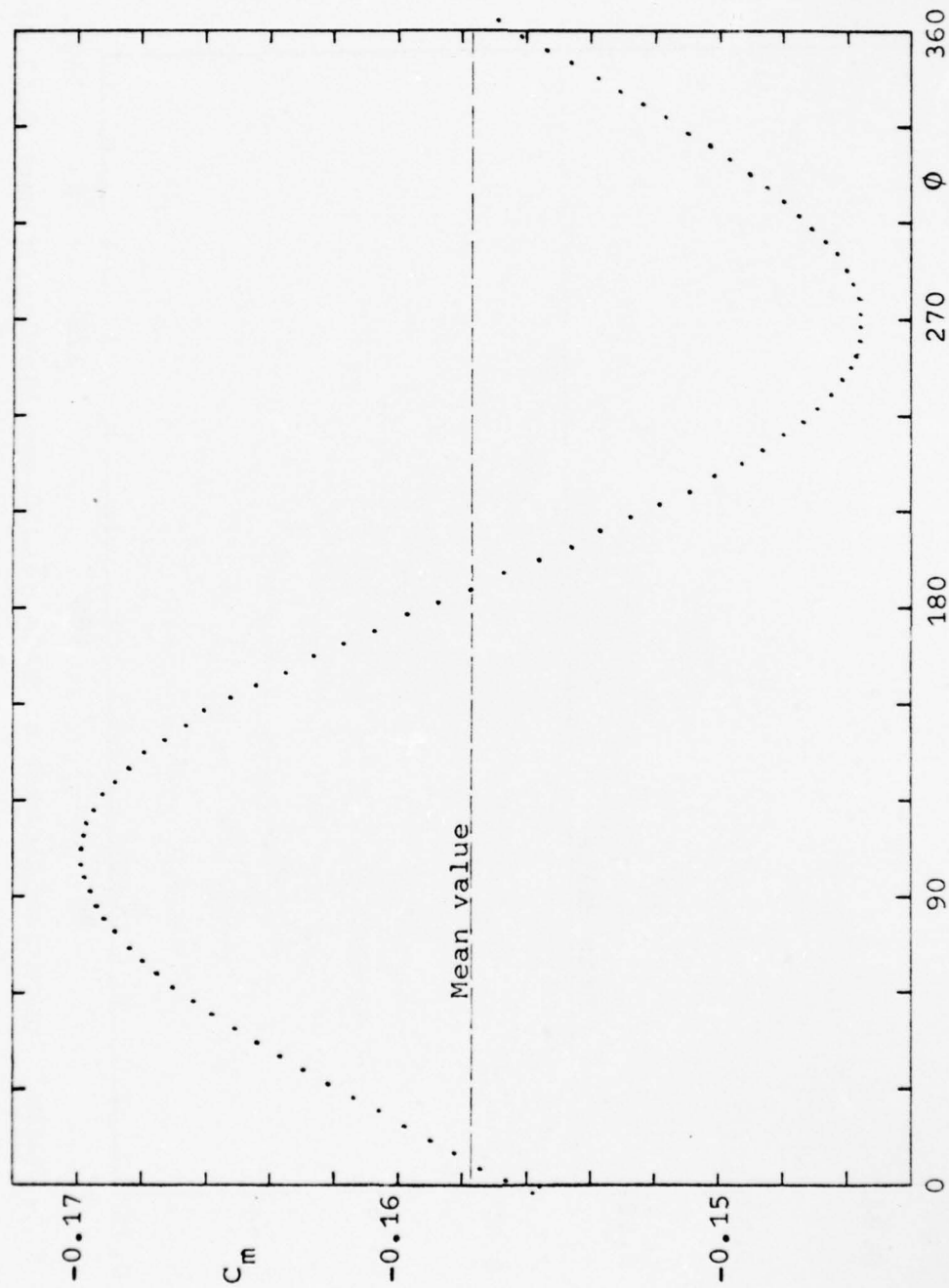


Figure 4. Pitching moment coefficient on NACA 64A410 oscillating in Mach 0.72 flow.

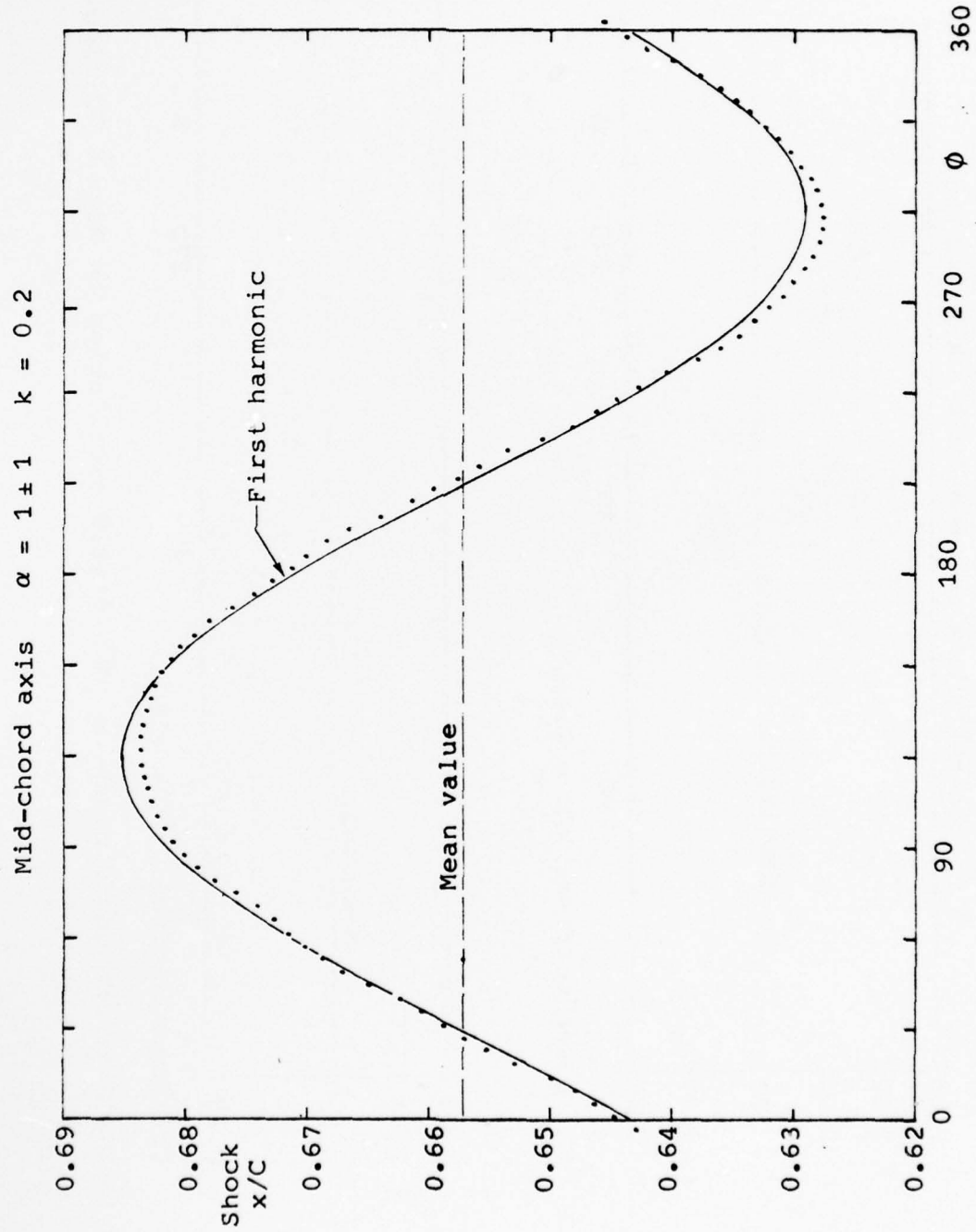
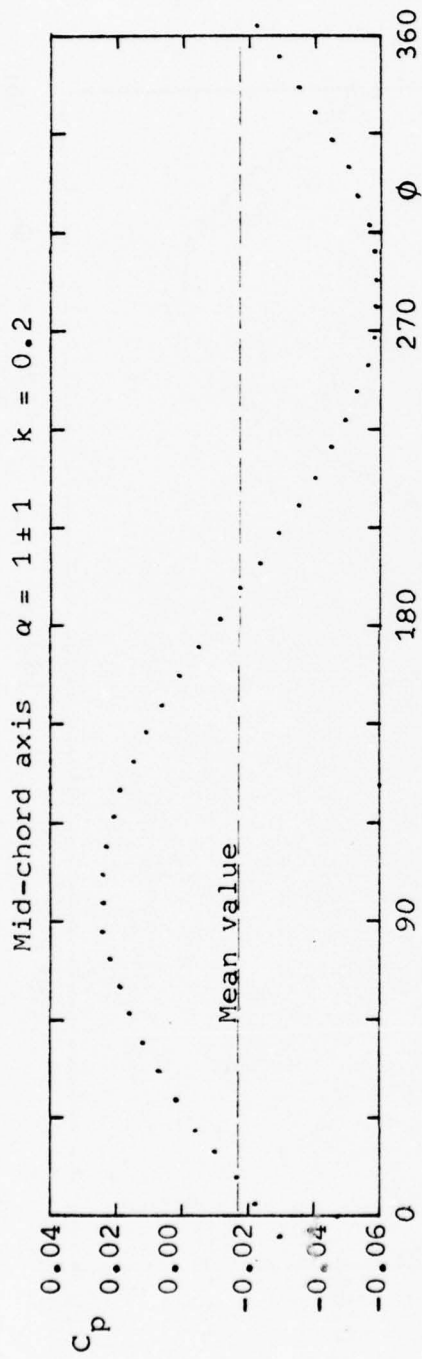
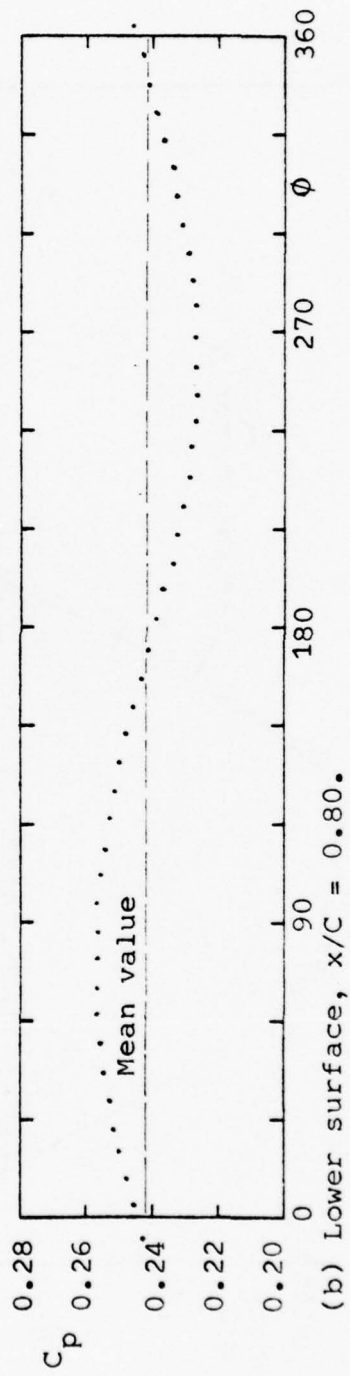


Figure 5. Shock location on NACA 64A410 oscillating in Mach 0.72 flow.

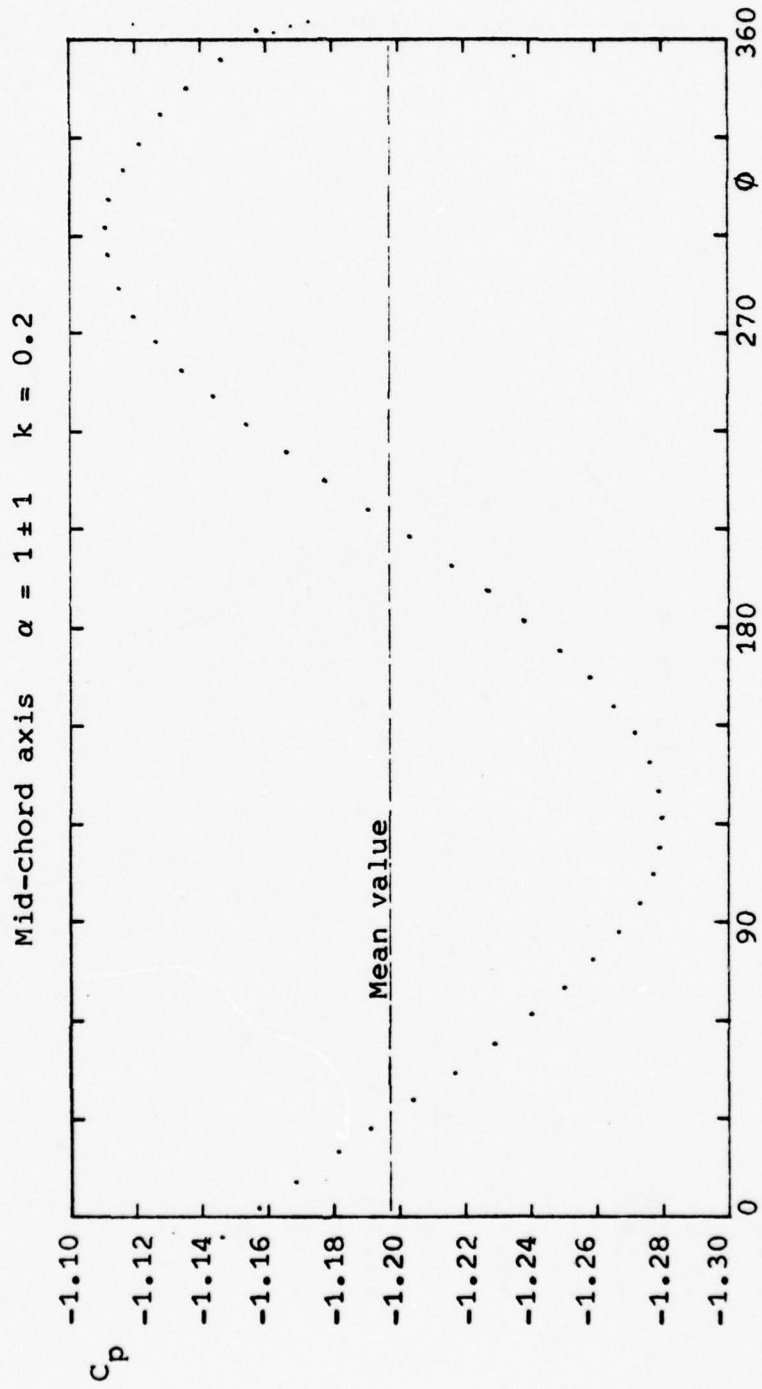


(a) Lower surface, $x/C = 0.40$.



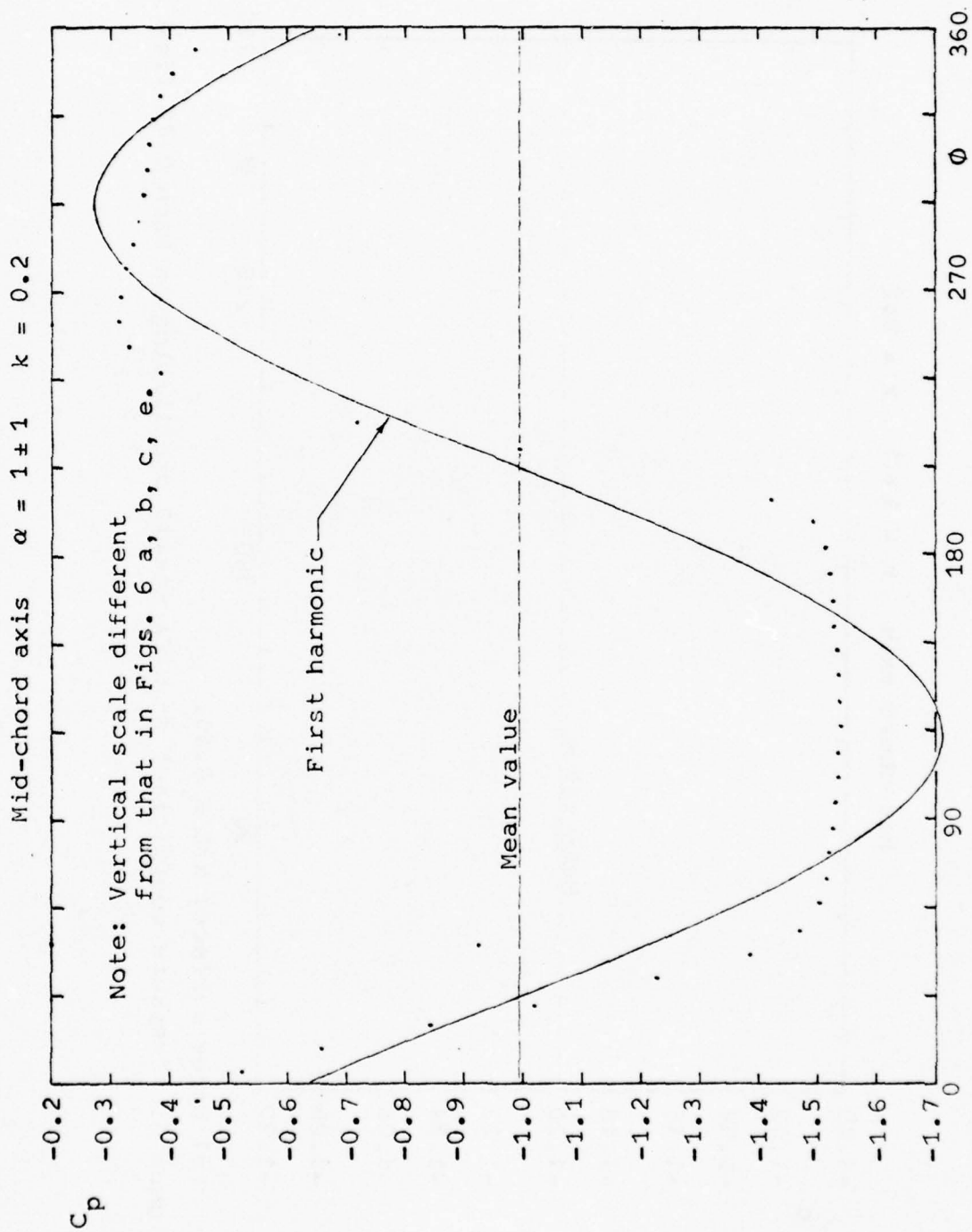
(b) Lower surface, $x/C = 0.80$.

Figure 6. Pressure coefficient on NACA 64A410 oscillating in Mach 0.72 flow.



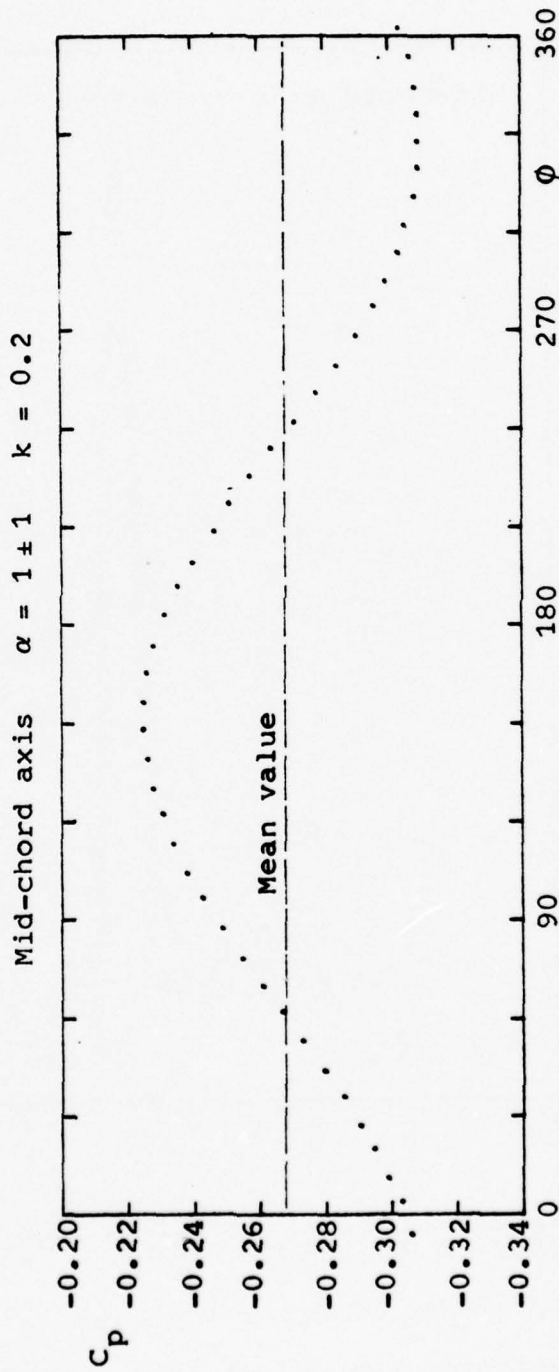
(c) Upper surface, $x/C = 0.40$.

Figure 6. Pressure coefficient on NACA 64A410 oscillating in Mach 0.72 flow.



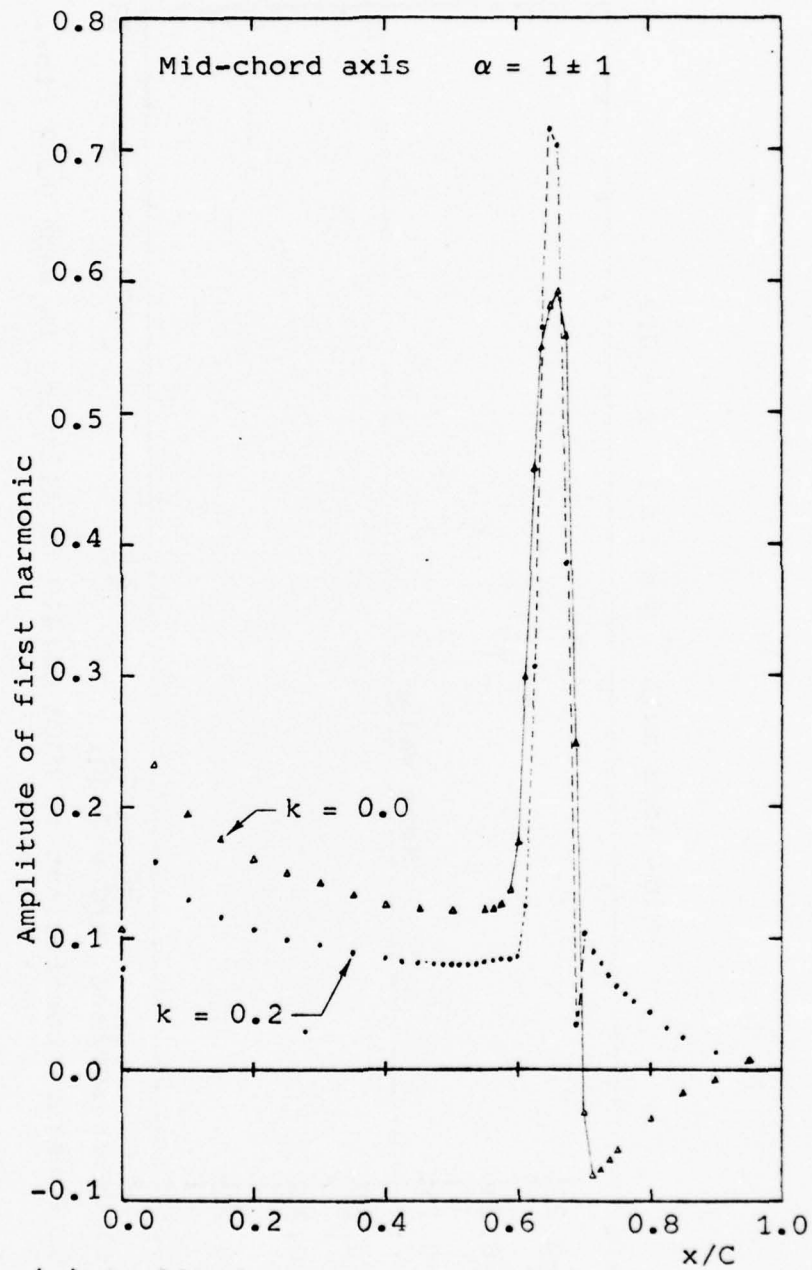
(d) Upper surface, $x/C = 0.65$.

Figure 6. Pressure coefficient on NACA 64A410 oscillating in Mach 0.72 flow.



(e) Upper surface, $x/C = 0.80$.

Figure 6. Pressure coefficient on NACA 641410 oscillating in Mach 0.72 flow.



(a) Amplitudes on upper surface.

Figure 7. Distribution of excursions in pressure coefficient on NACA 64A410 oscillating in Mach 0.72 flow.

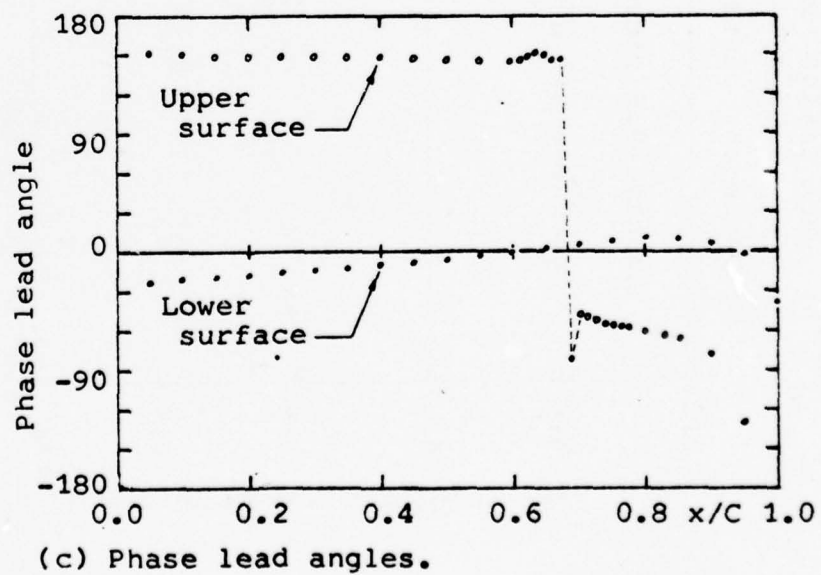
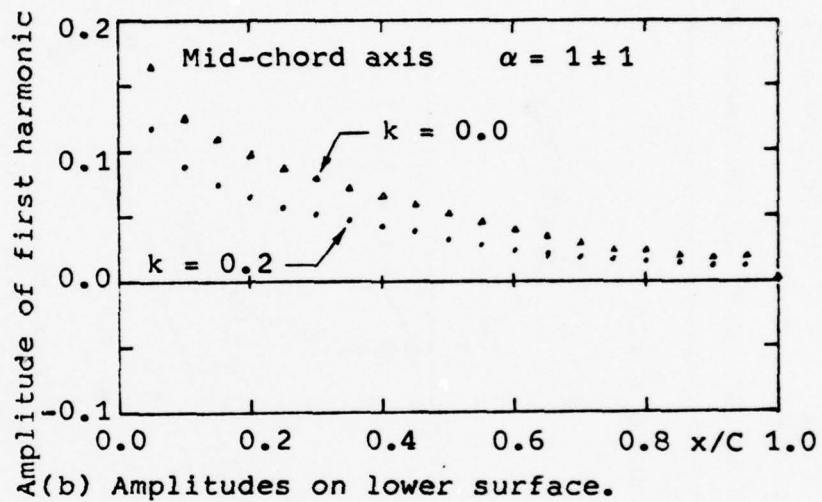


Figure 7. Distribution of excursions in pressure coefficient on NACA 64A410 oscillating in Mach 0.72 flow.

NACA 64A410 Mach 0.72 = 2 Midchord axis
 $C_N(\phi) = S_1 \sin(\phi) + C_1 \cos(\phi)$
 Response per radian of pitch oscillation amplitude

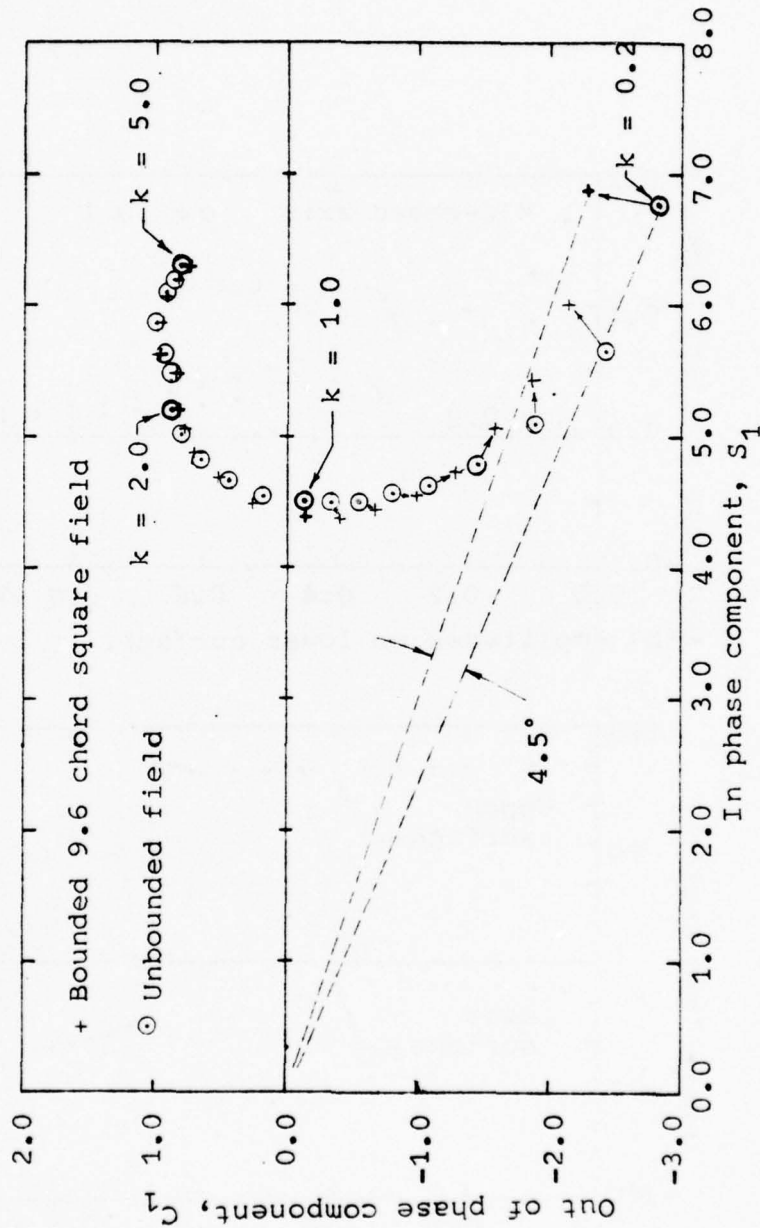


Figure 8. Comparison of normal force responses expected in bounded and unbounded computational fields.

NACA 64A410 Mach 0.72 = 2 Midchord axis

$$C_m(\phi) = S_1 \sin(\phi) + C_1 \cos(\phi)$$

Response per radian of pitch oscillation amplitude
C/4 reference axis, nose up positive

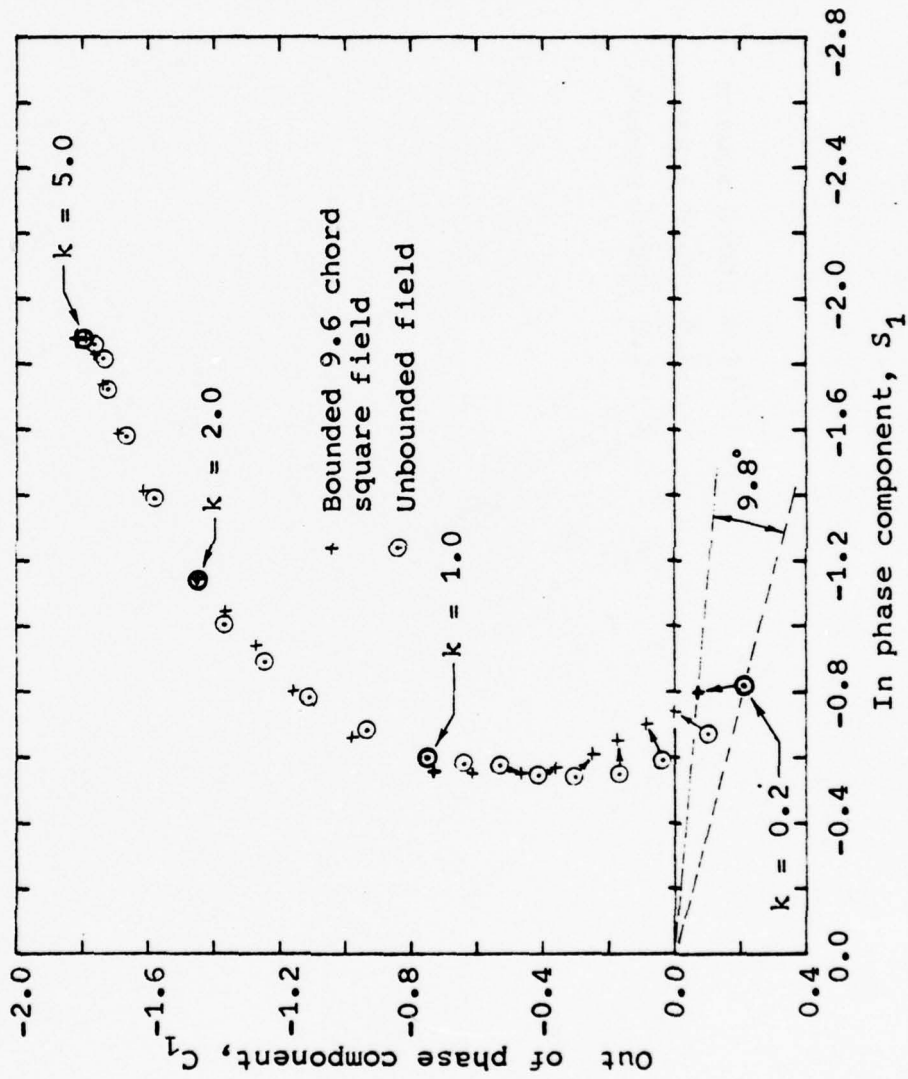


Figure 9. Comparison of pitching moment responses expected in bounded and unbounded computational fields.

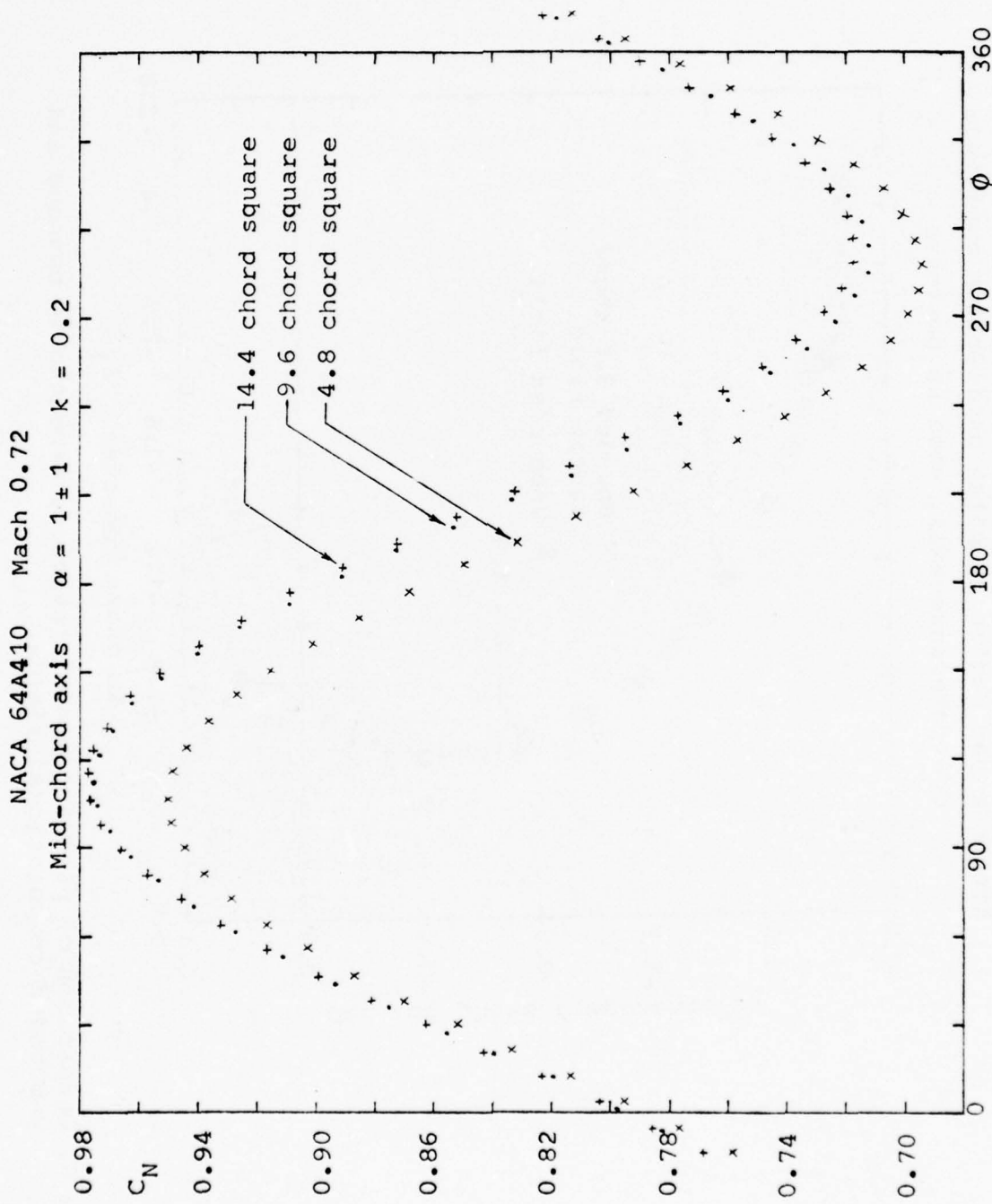


Figure 10. Effect of computation field size on normal force.

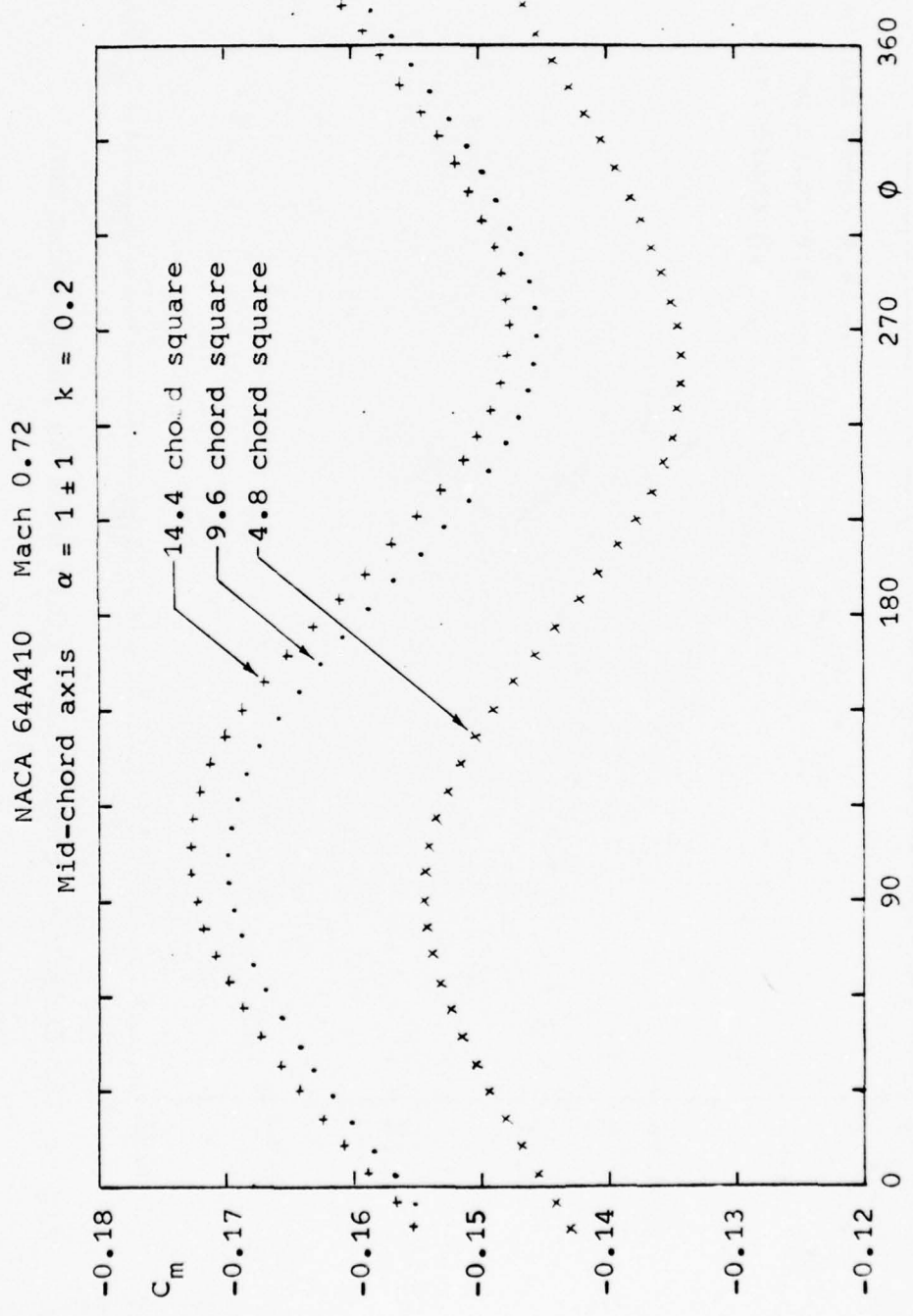


Figure 11. Effect of computation field size on pitching moment.

NACA 64A410 Mach 0.72
Mid-chord axis $\alpha = 1 \pm 1$ $k = 0.2$

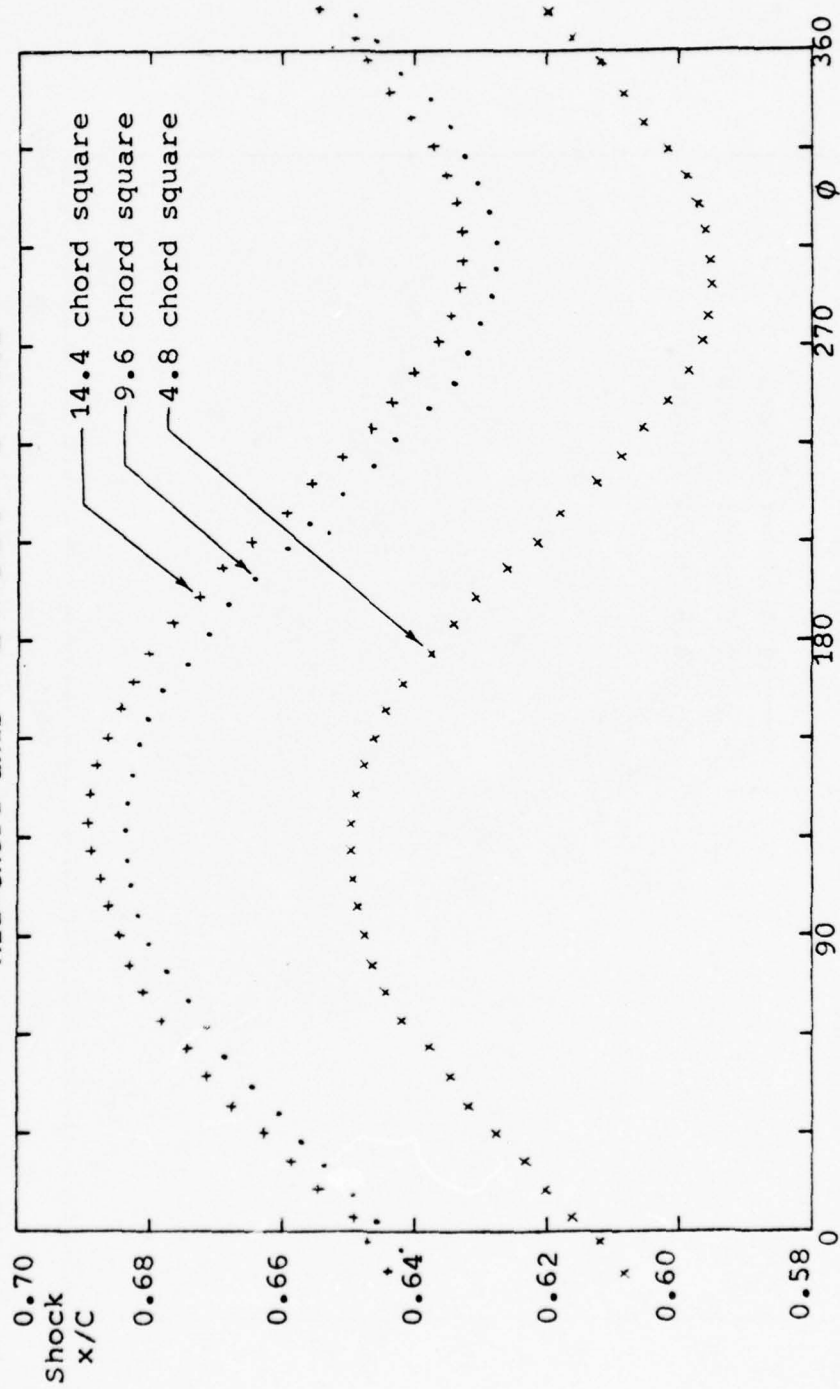


Figure 12. Effect of computation field size on shock location.

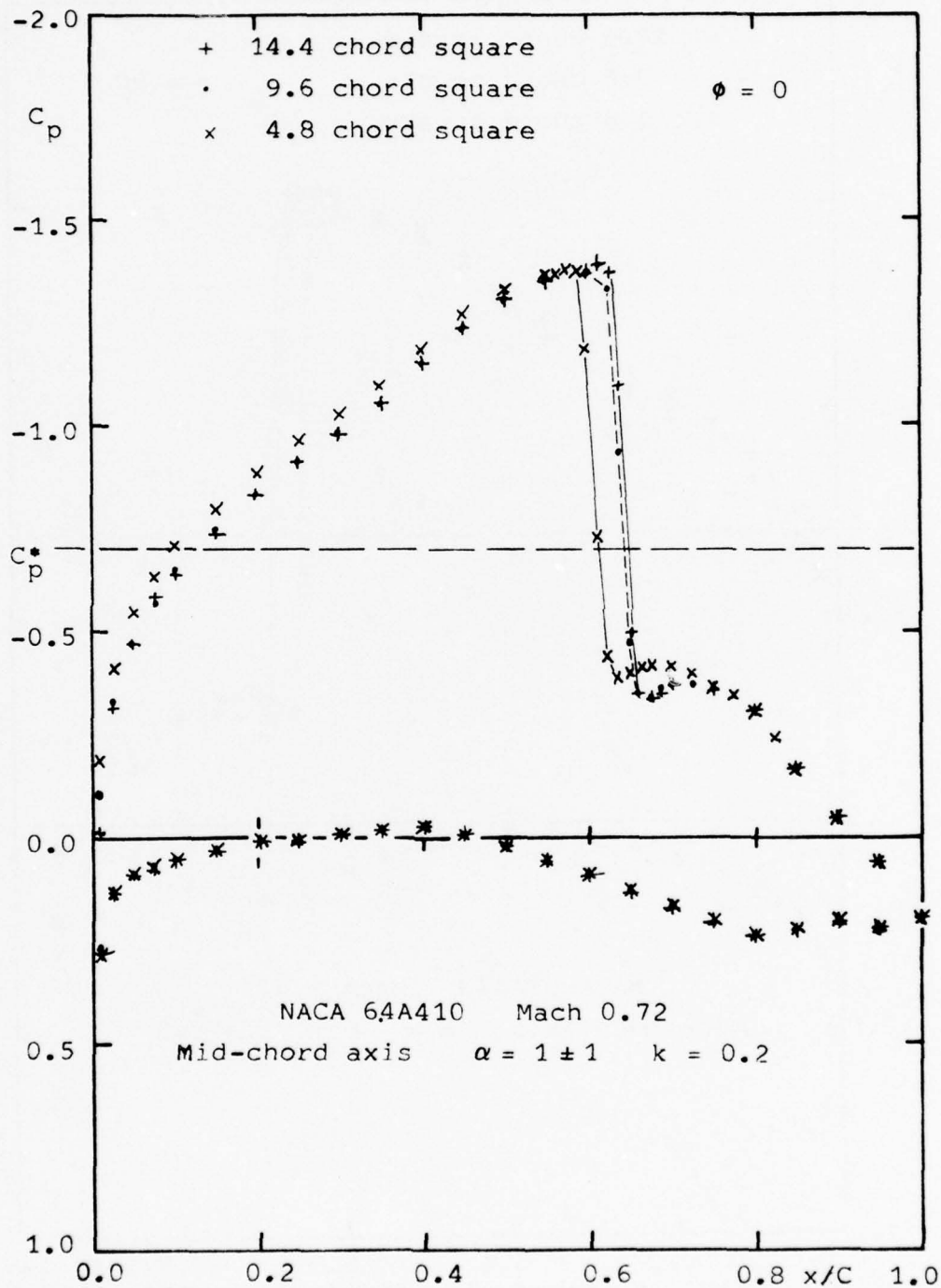


Figure 13. Effect of computation field size on pressure distribution. (a) $\phi = 0$.

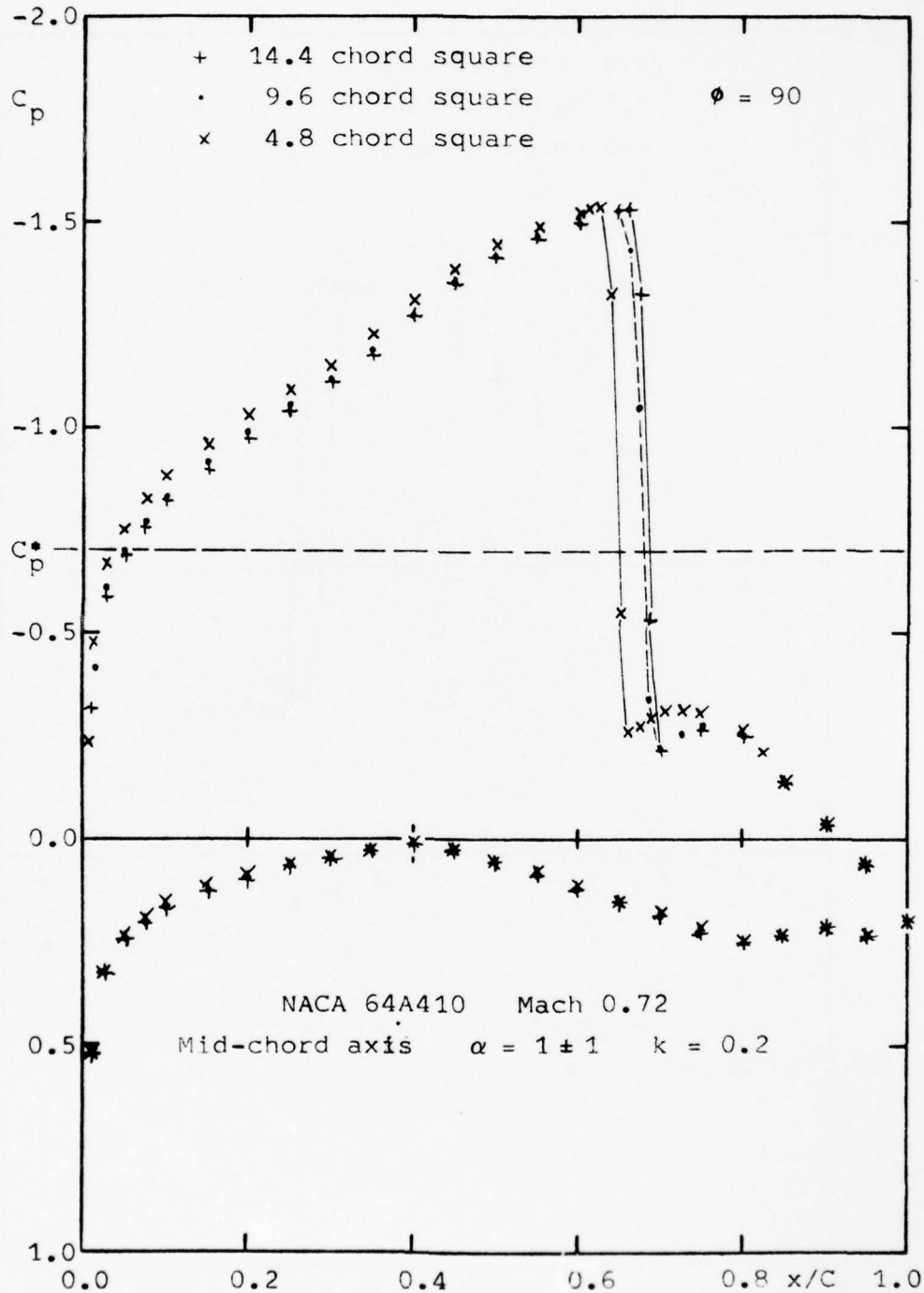


Figure 13. Effect of computation field size on pressure distribution. (b) $\phi = 90$.

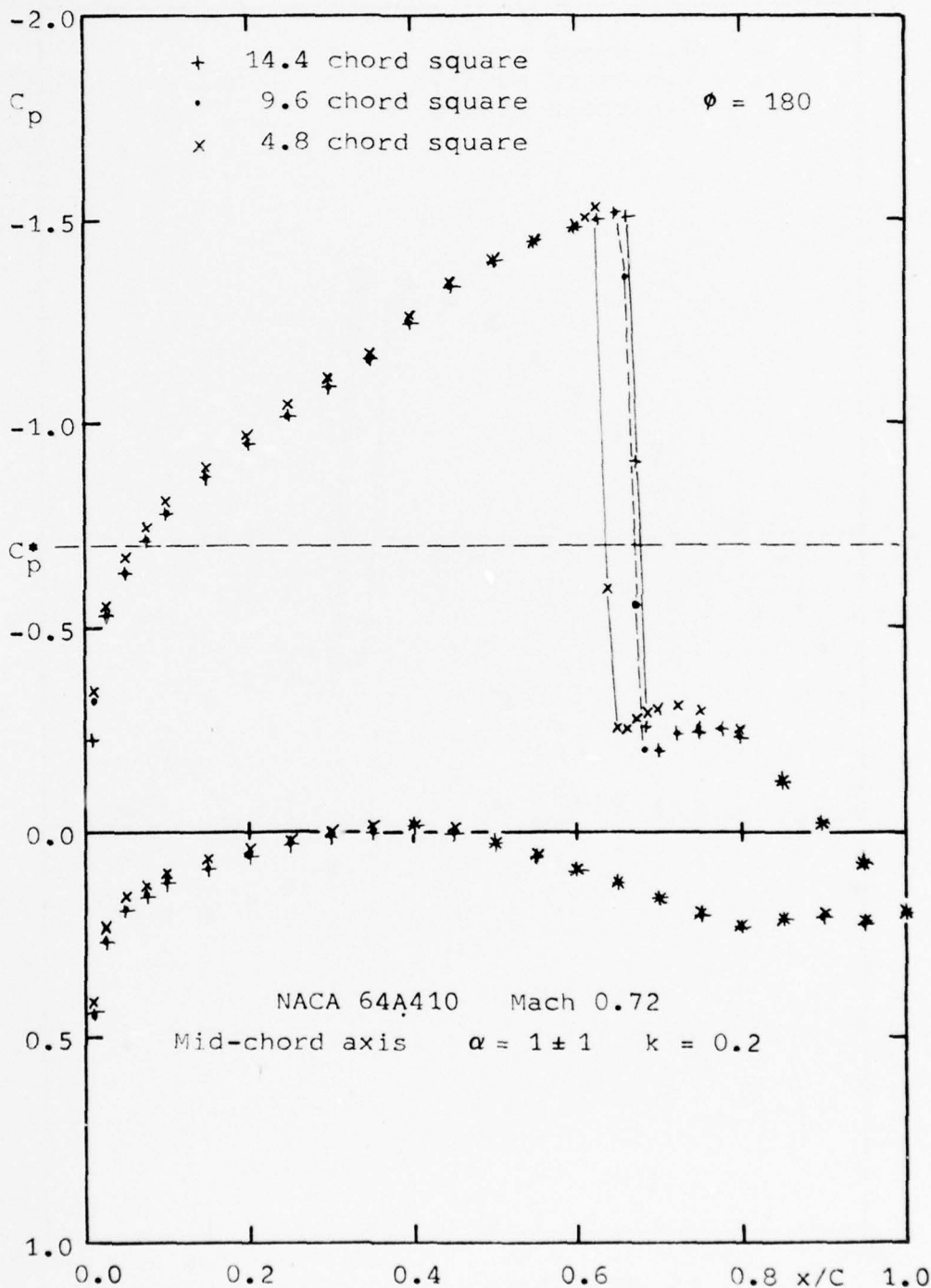


Figure 13. Effect of computation field size on pressure distribution. (c) $\phi = 180$.

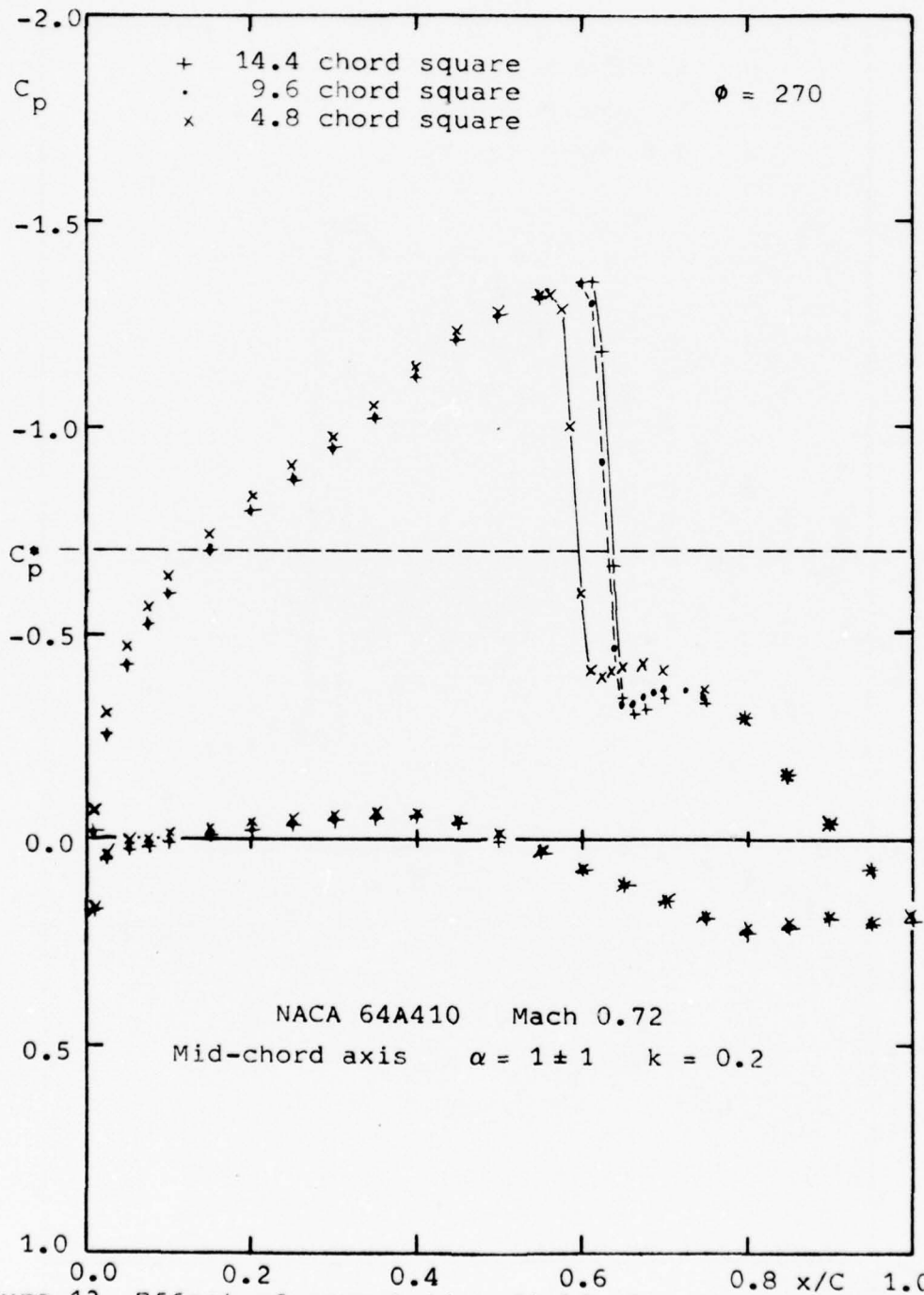
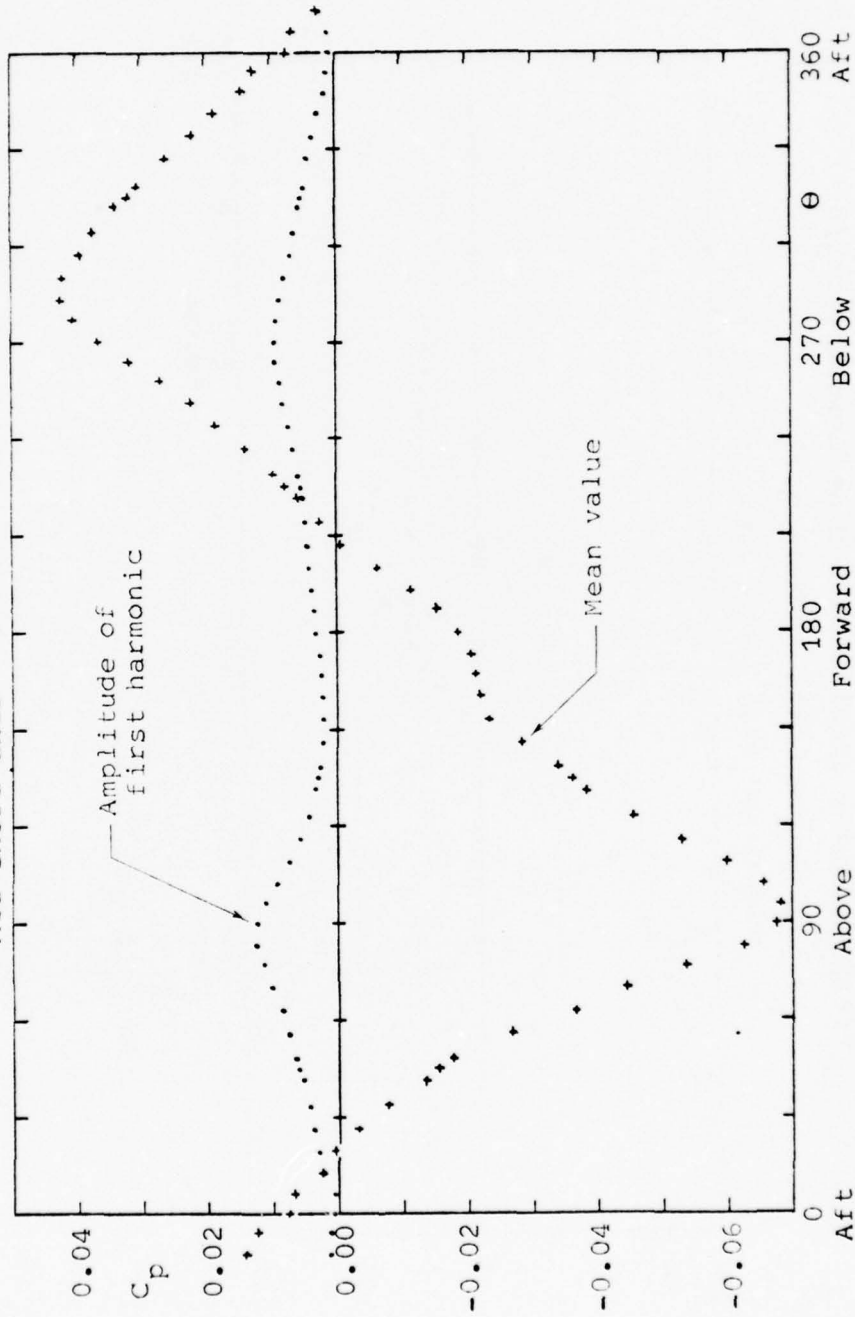


Figure 13. Effect of computation field size on pressure distribution. (d) $\phi = 270$.

Pressures on a circle 3.6 chords from mid-chord

NACA 64A410 Mach 0.72

Mid-chord axis $\alpha = 1 \pm 1$ $k = 0.2$



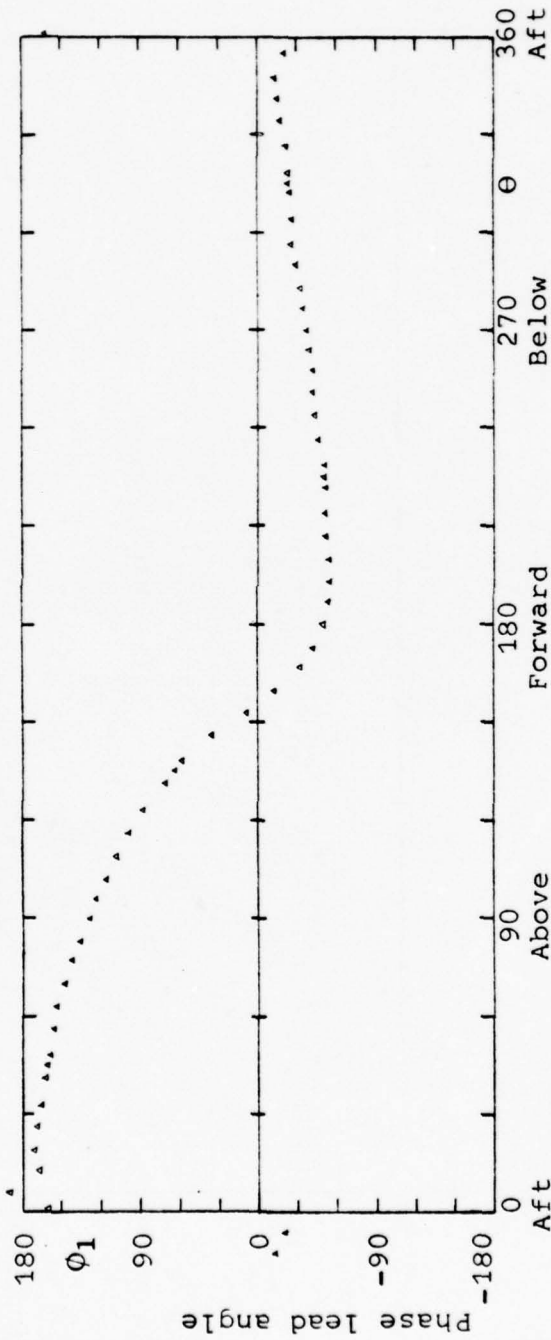
(a) Mean pressures and amplitudes of excursions.

Figure 14. Pressures in outer field.

Pressures on a circle 3.6 chords from mid-chord

NACA 64A410 Mach 0.72

Mid-chord axis $\alpha = 1 \pm 1$ $k = 0.2$



(b) Phase lead angle.

Figure 14. Pressures in outer field.

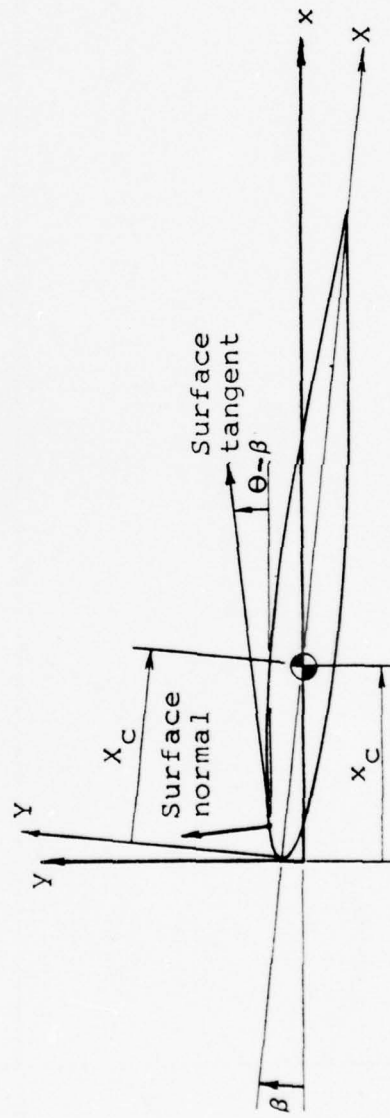
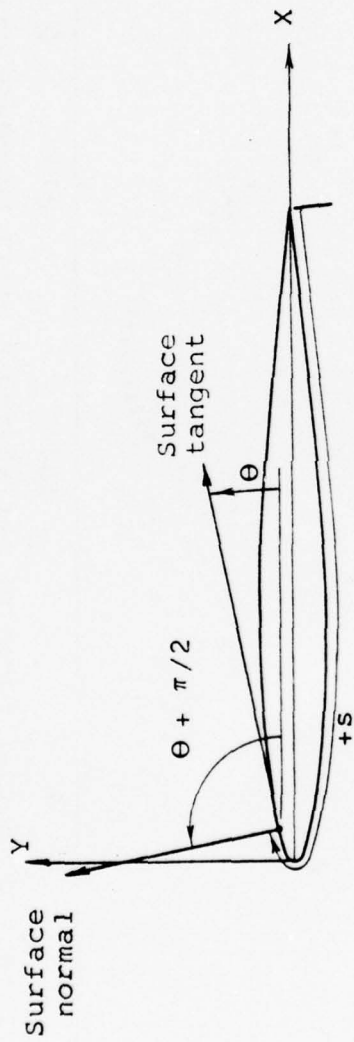


Figure 15. Airfoil-fixed and space-fixed coordinate systems.

NACA 64A010 Mach 0.80
Plunging oscillations $\alpha = 0$ $k = 0.4$

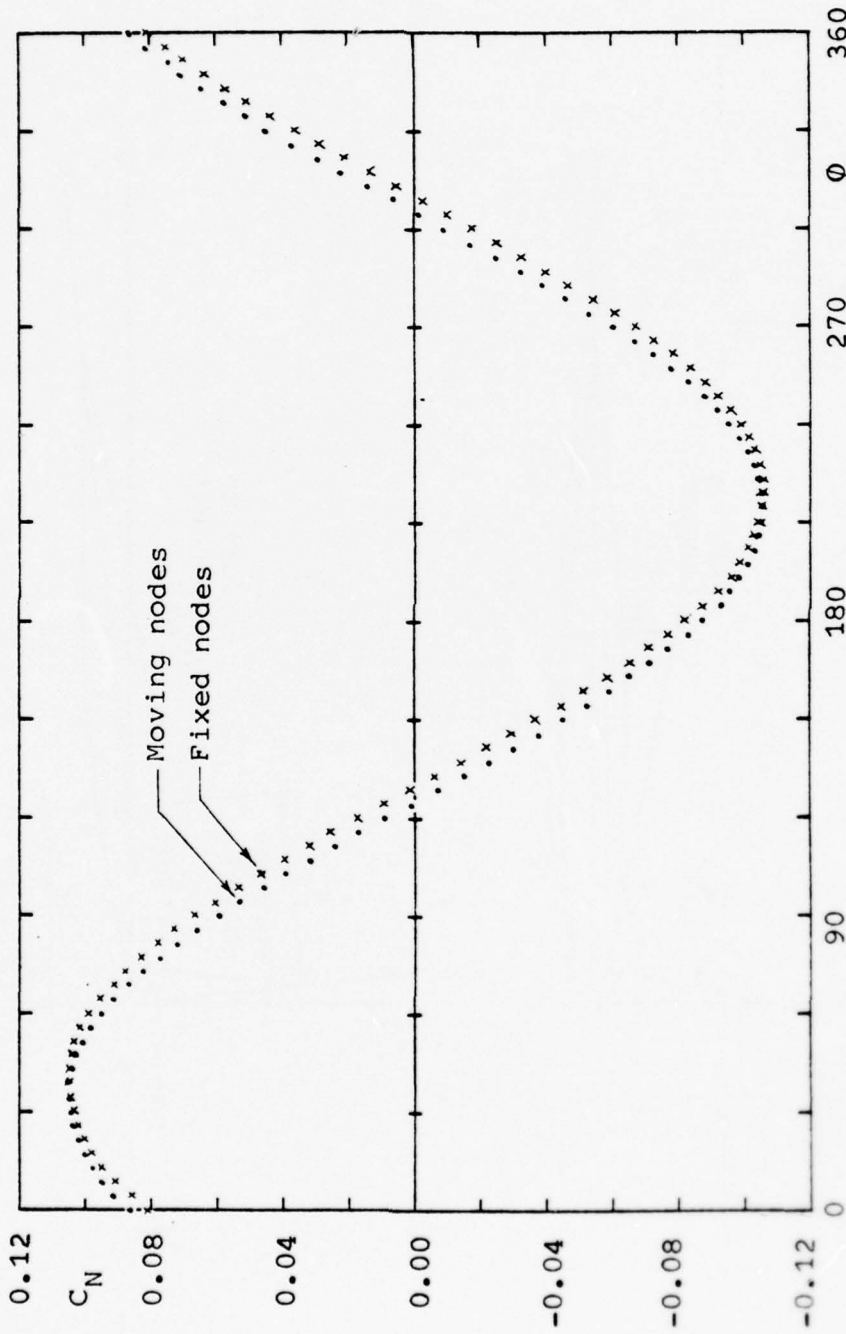


Figure 16. Effect on normal force of satisfying airfoil boundary conditions at fixed nodes.

NACA 64A010 Mach 0.80

Plunging oscillations $\alpha = 0$ $k = 0.4$

C/4 reference axis Nose up moment positive

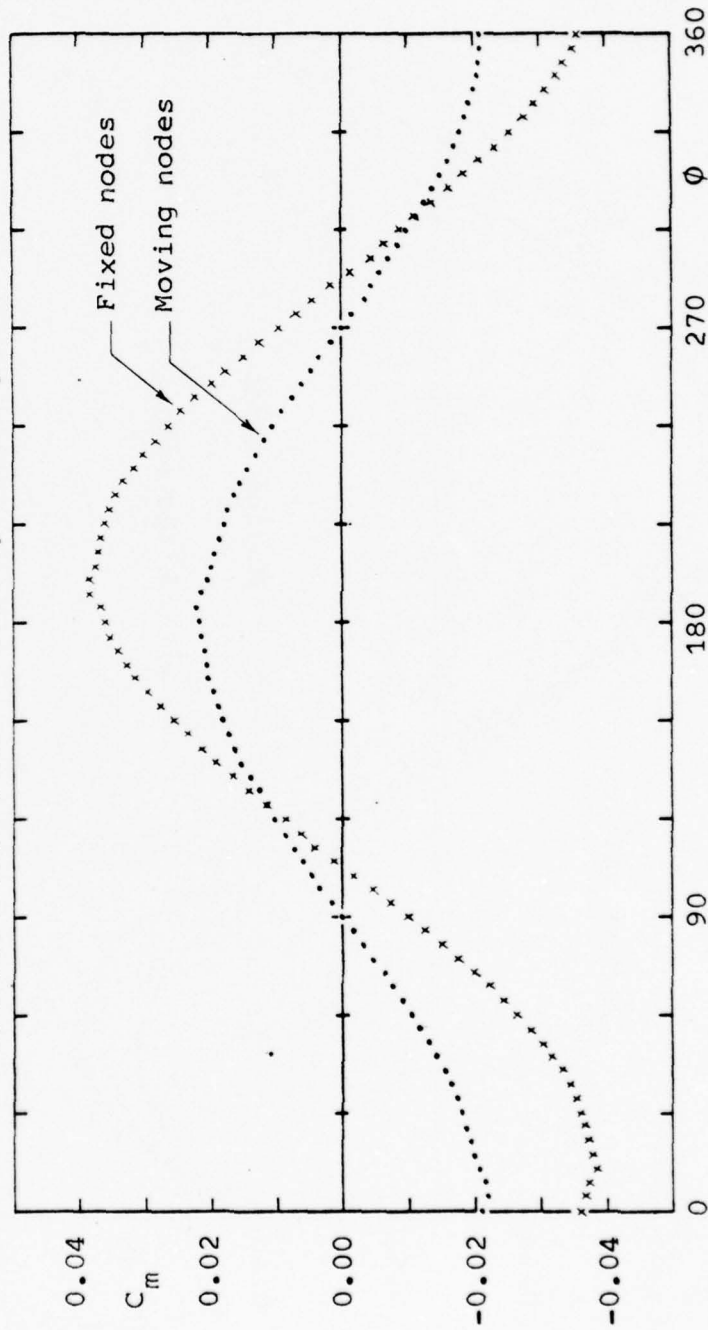


Figure 17. Effect on pitching moment of satisfying airfoil boundary conditions at fixed nodes.

NACA 64A010 Mach 0.80
 Plunging oscillations $\alpha = 0$ $k = 0.4$

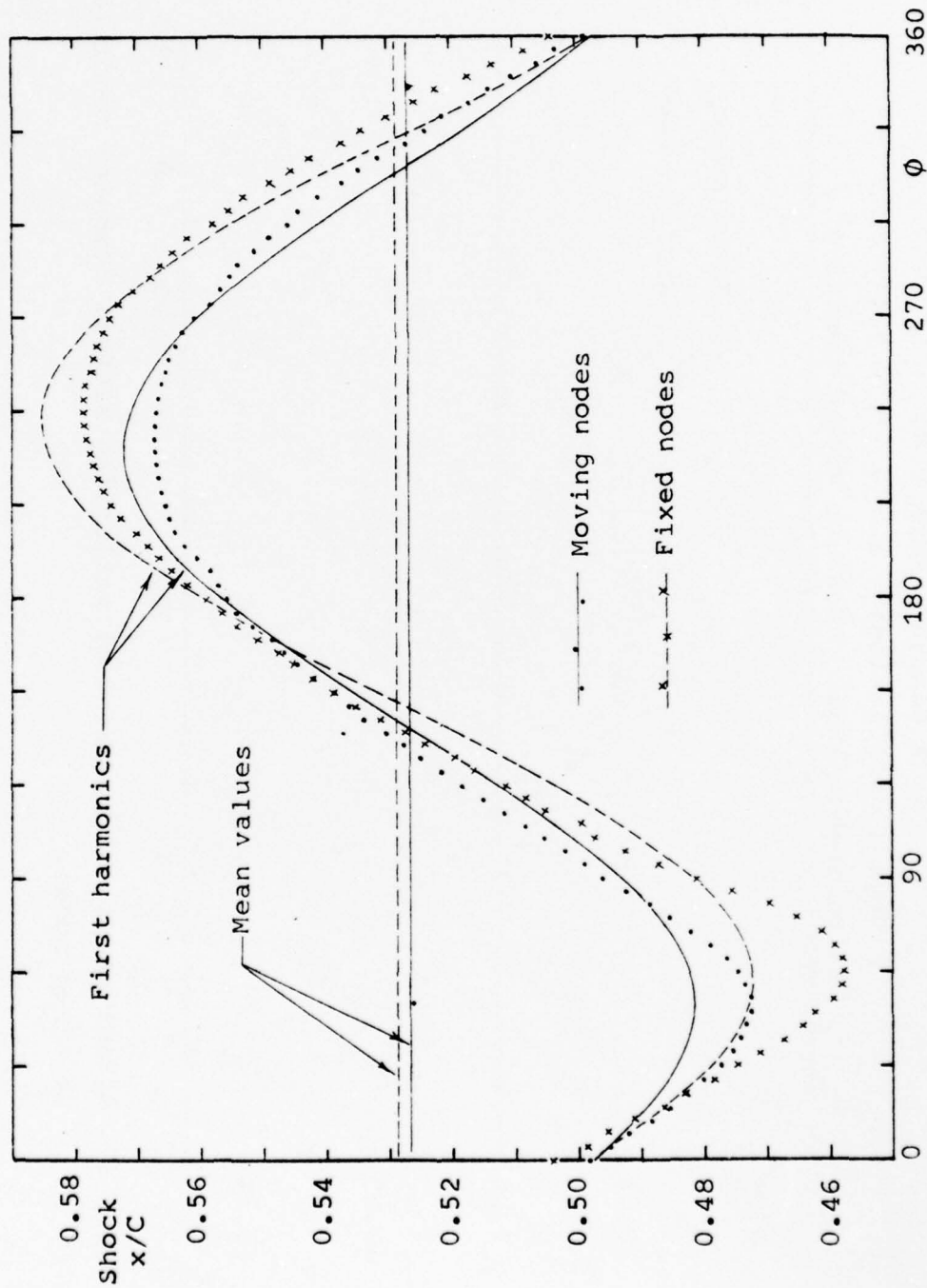


Figure 18. Effect on position of lower surface shock of satisfying airfoil boundary conditions at fixed nodes.

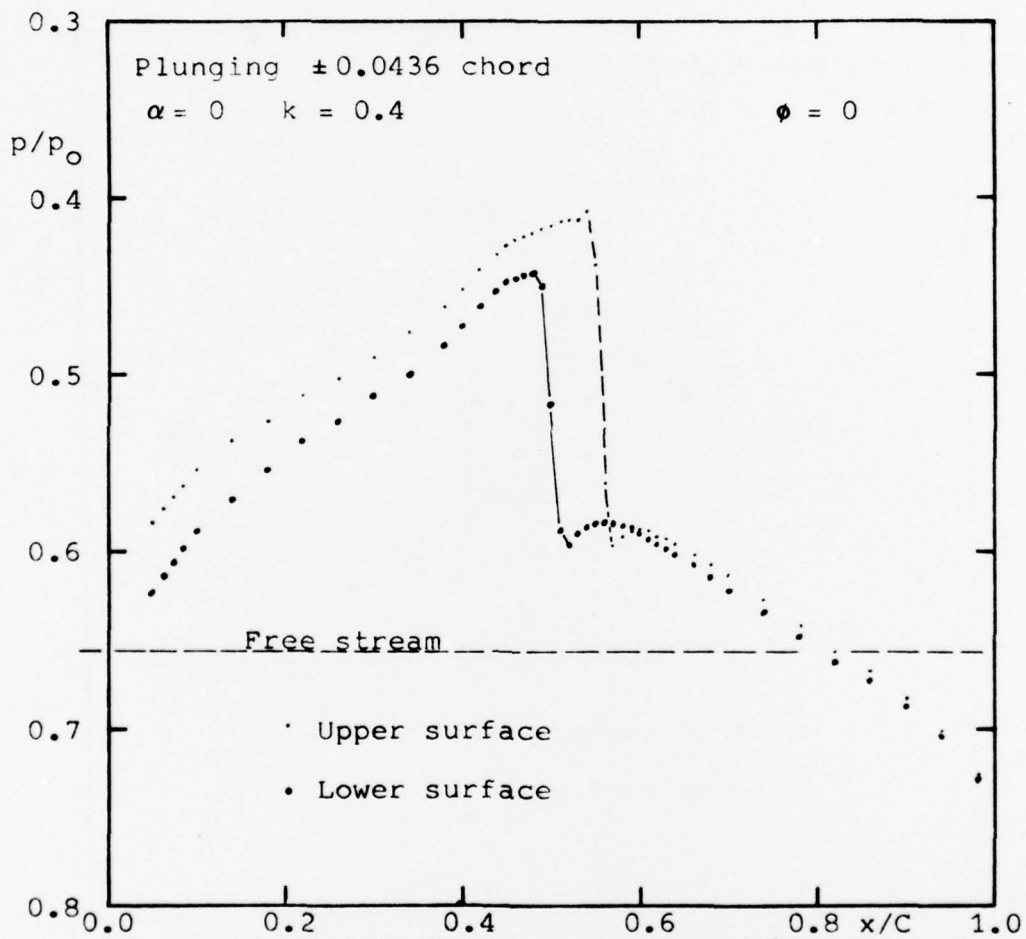


Figure 19. Pressure distribution on NACA 64A010 oscillating in Mach 0.80 flow. (a) $\phi = 0$.

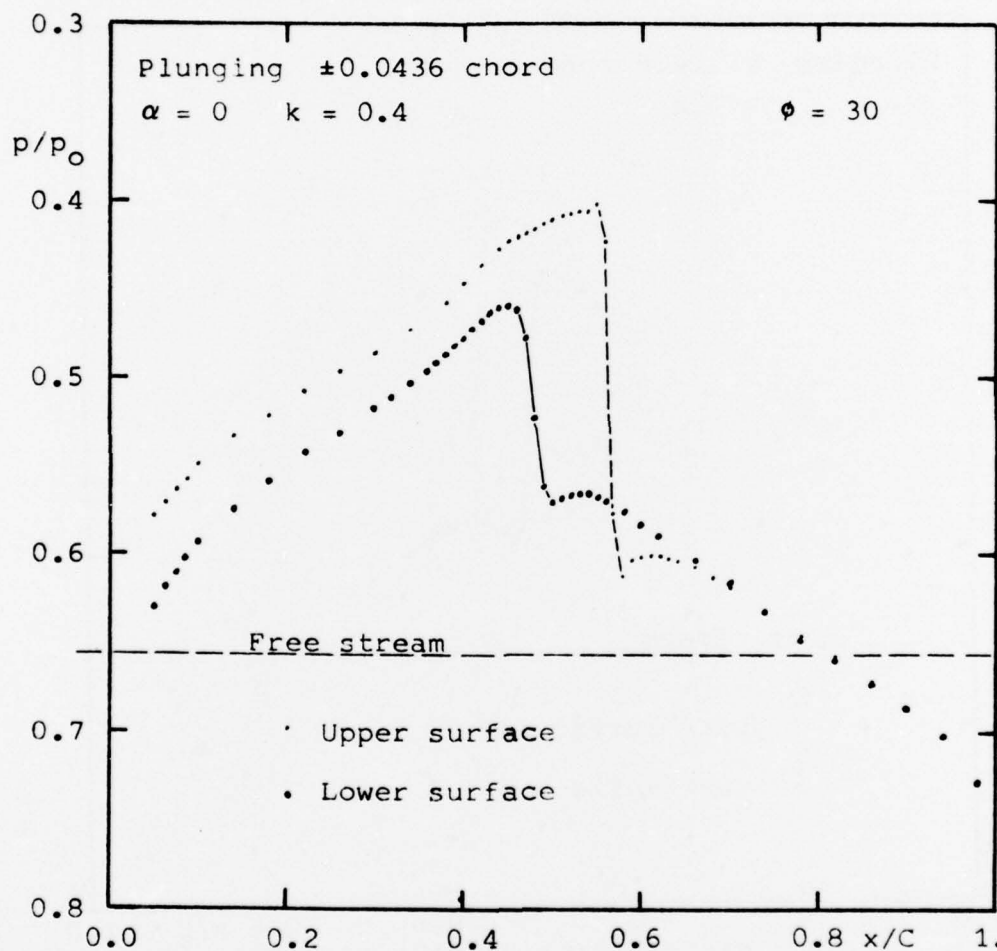


Figure 19. Pressure distribution on NACA 64A010 oscillating in Mach 0.80 flow. (b) $\phi = 30$.

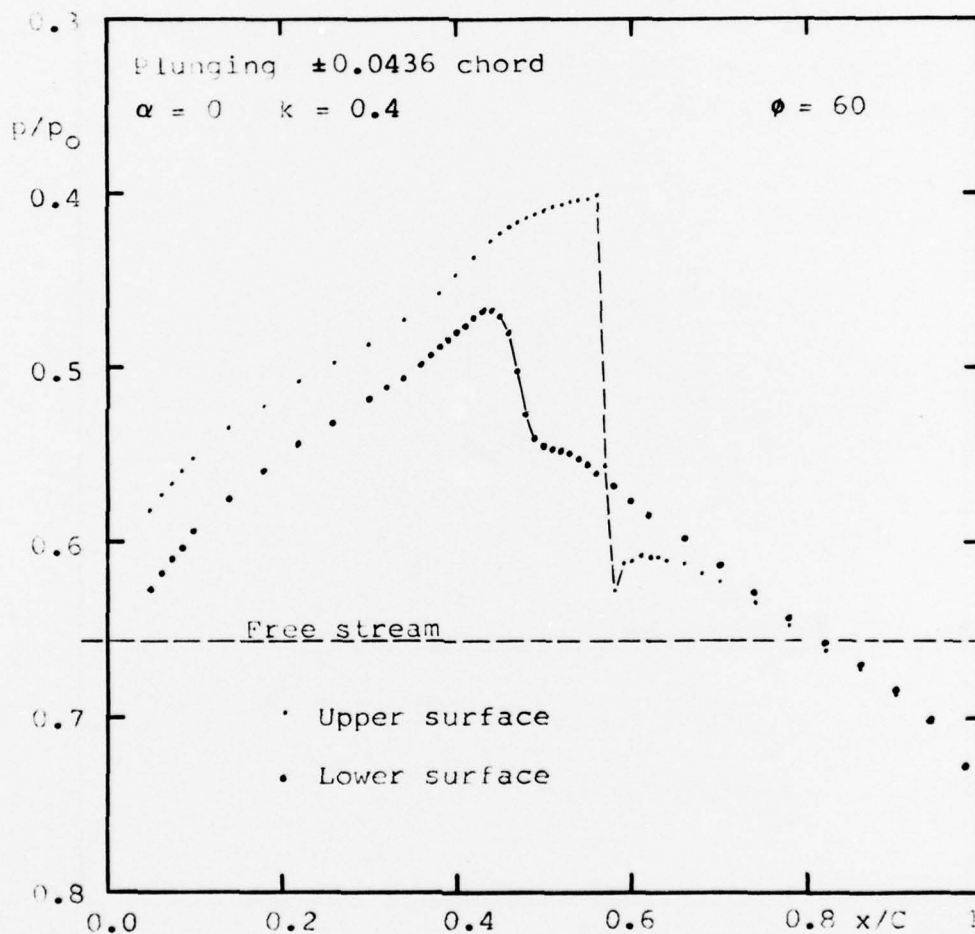


Figure 19. Pressure distribution on NACA 64A010 oscillating in Mach 0.80 flow. (c) $\phi = 60$.

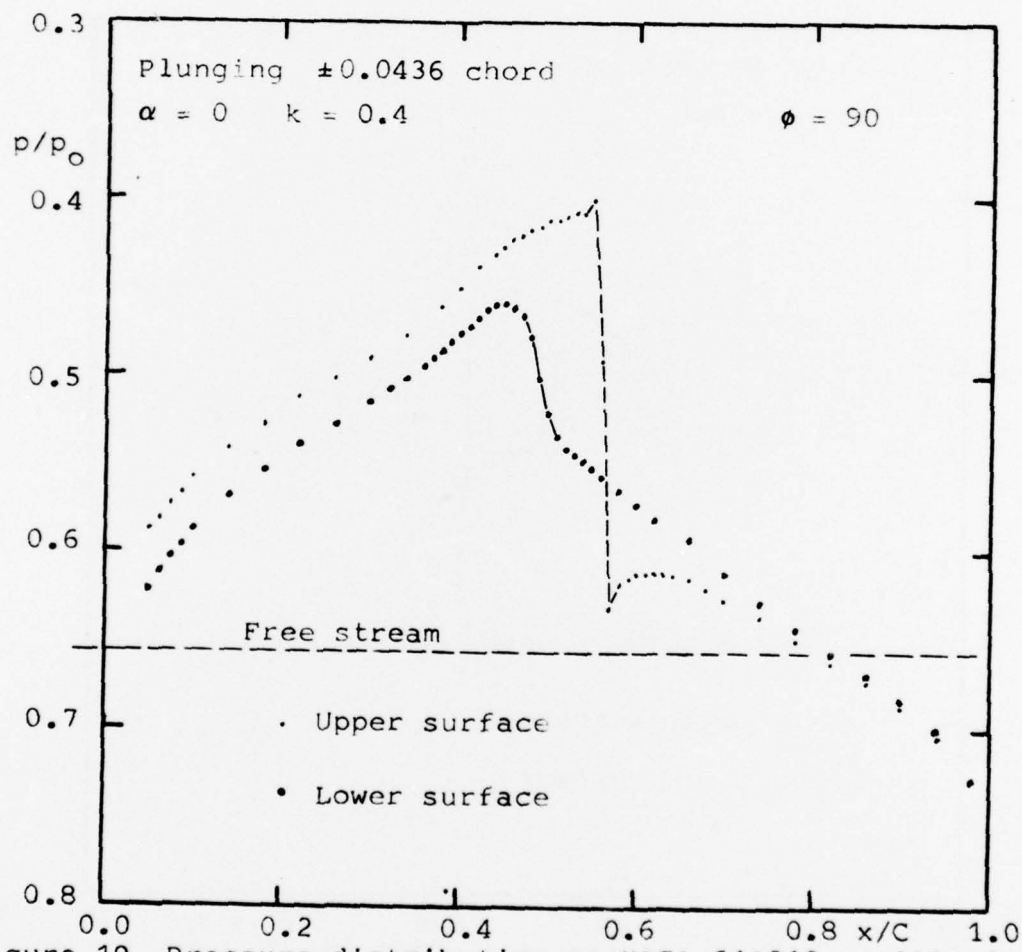


Figure 19. Pressure distribution on NACA 64A010 oscillating in Mach 0.80 flow. (d) $\phi = 90$.

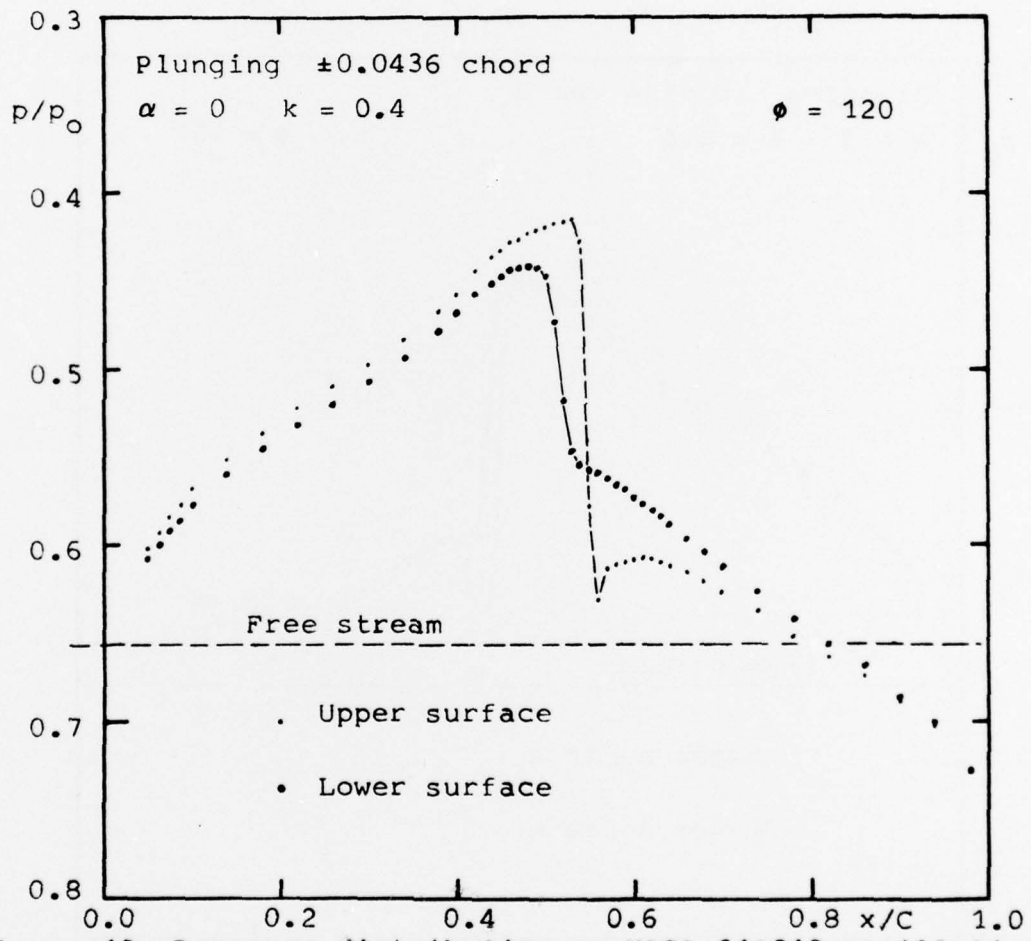


Figure 19. Pressure distribution on NACA 64A010 oscillating in Mach 0.80 flow. (e) $\phi = 120$.

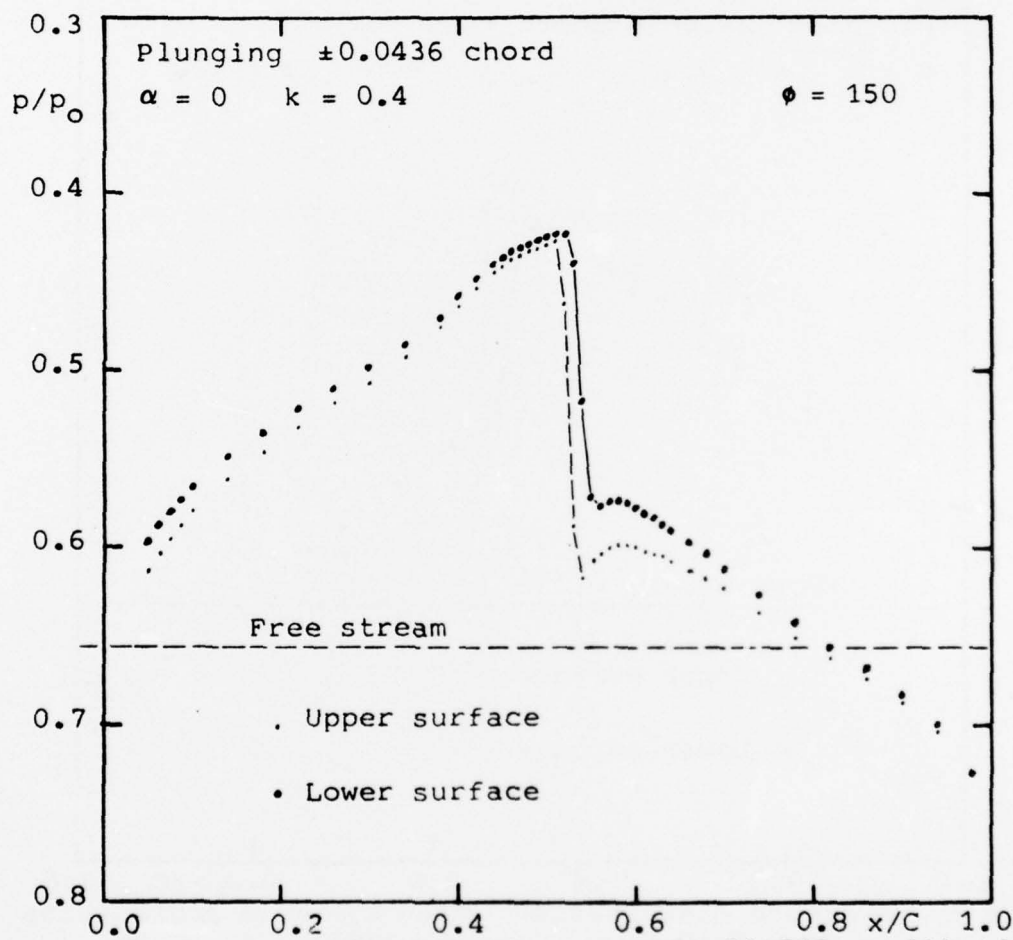
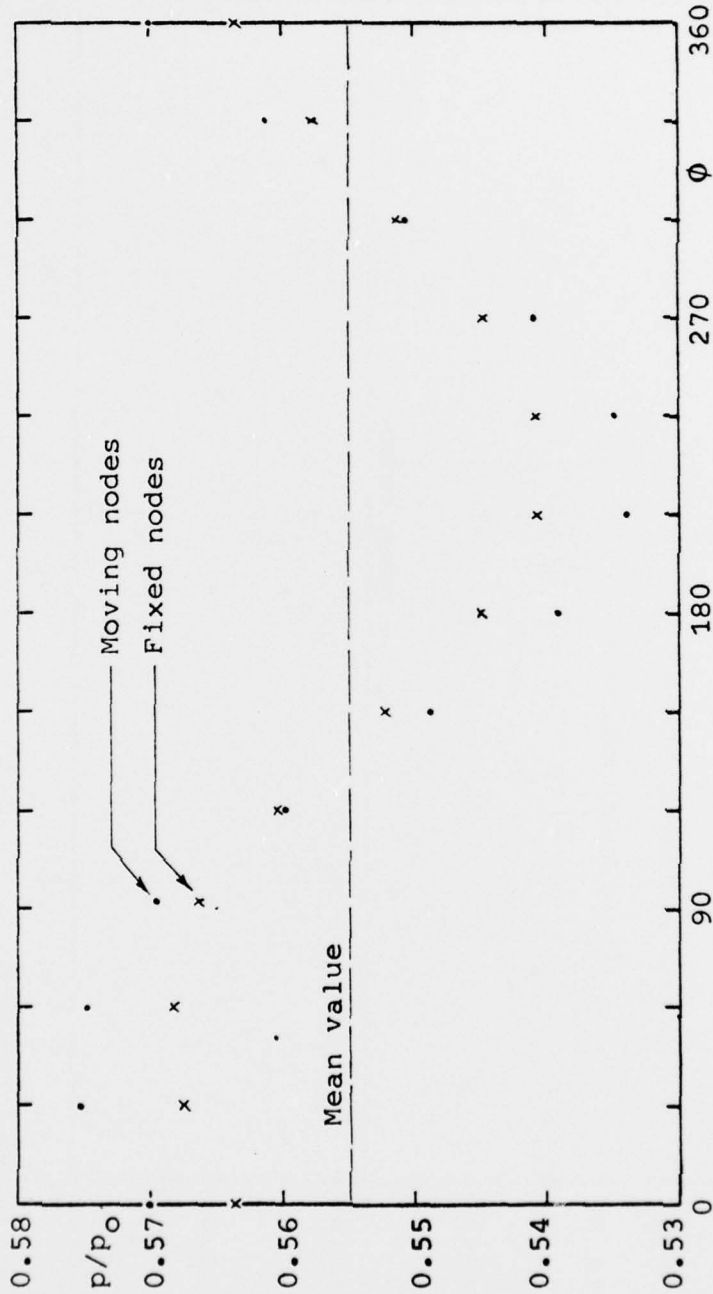


Figure 19. Pressure distribution on NACA 64A010 oscillating in Mach 0.80 flow. (f) $\phi = 150$.

NACA 64A010 Mach 0.80

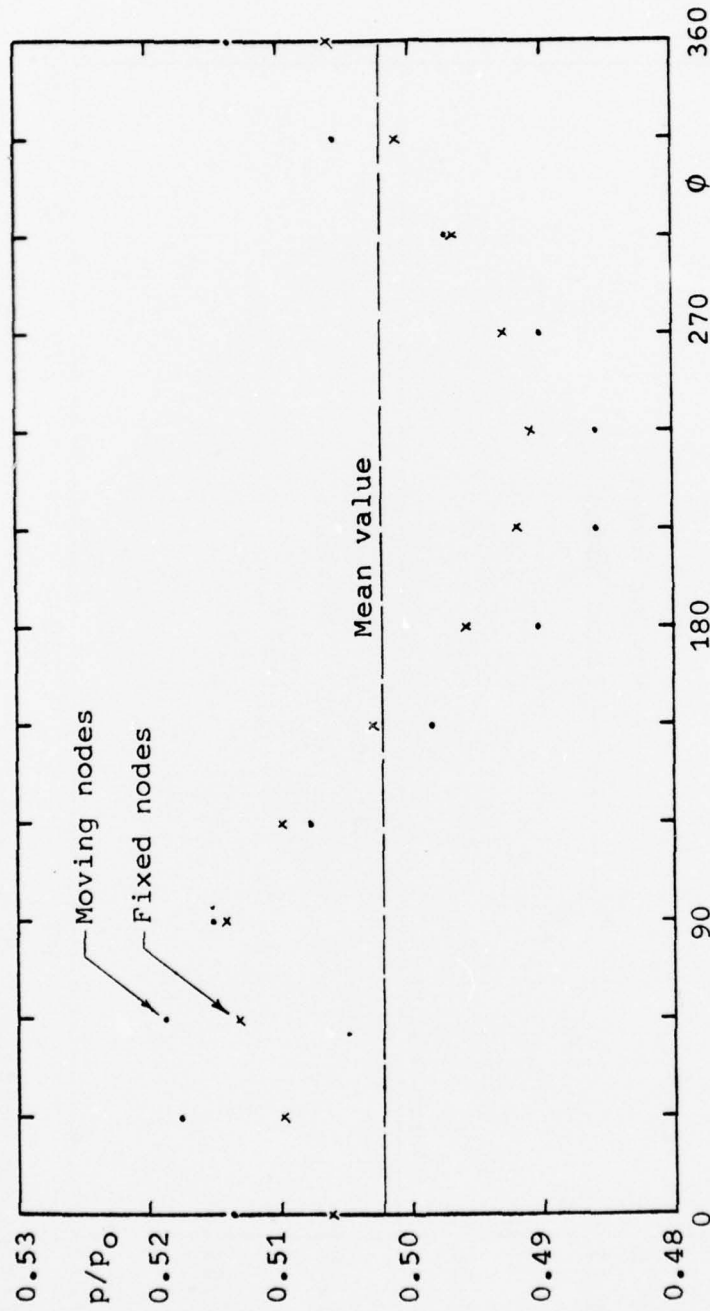
Plunging oscillations $\alpha = 0$ $k = 0.4$



(a) Lower surface, $x/C \approx 0.14$.

Figure 20. Effect on pressure of satisfying airfoil boundary conditions at fixed nodes.

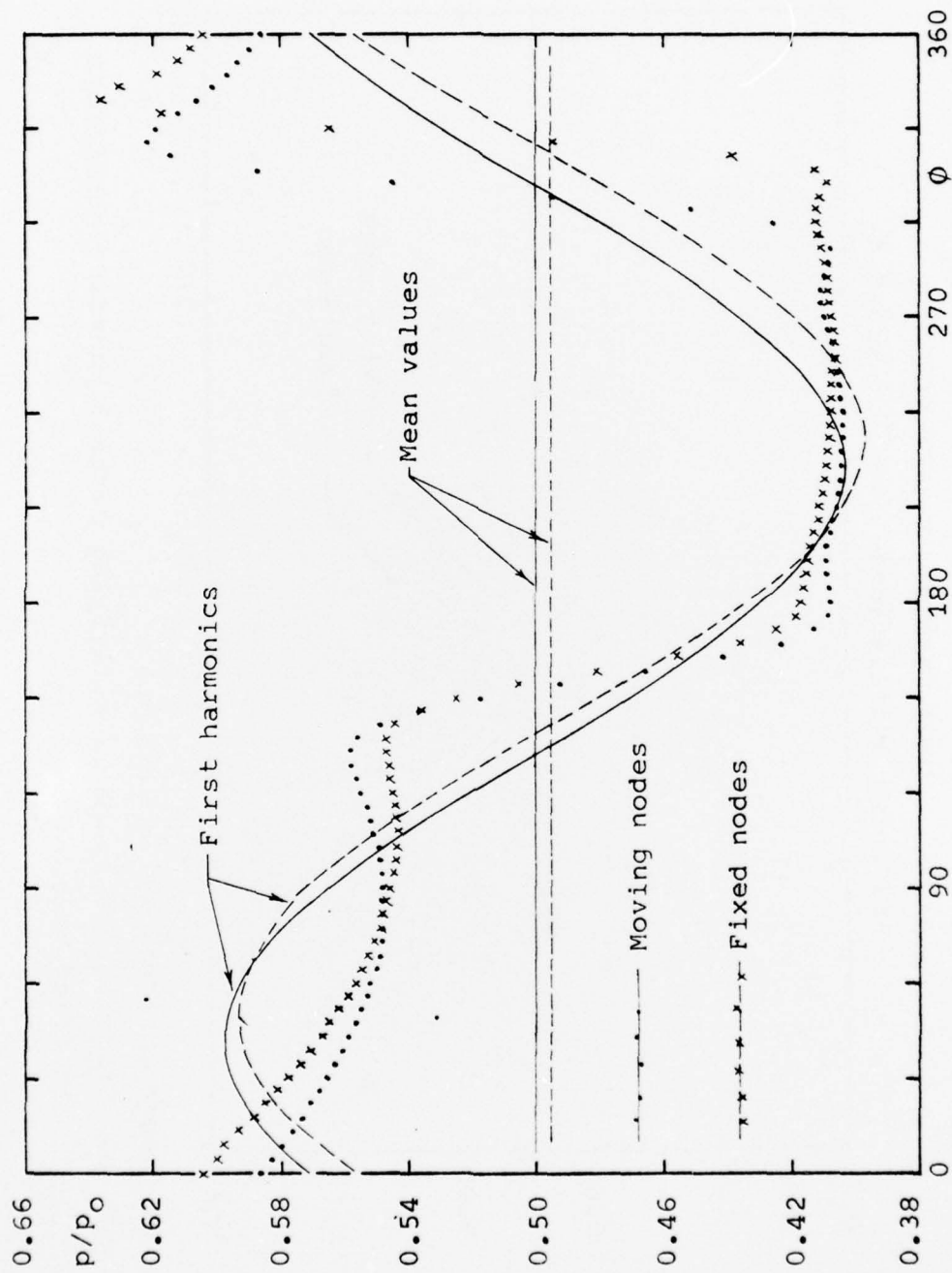
NACA 64A010 Mach 0.80
 Plunging oscillations $\alpha = 0$ $k = 0.4$



(b) Lower surface, $x/C = 0.30$.

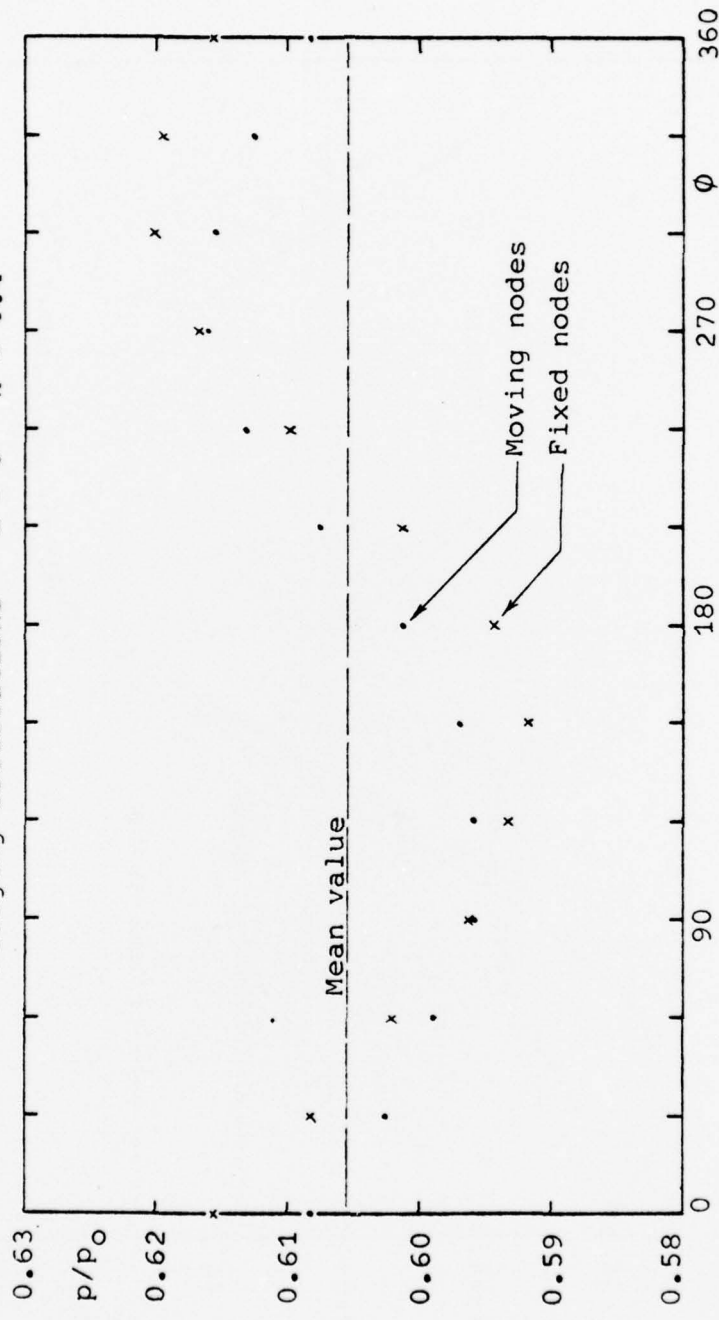
Figure 20. Effect on pressure of satisfying airfoil boundary conditions at fixed nodes.

NACA 64A010 Mach 0.80
 Plunging oscillations $\alpha = 0$ $k = 0.4$



(c) Lower surface, $x/C = 0.54$.
 Figure 20. Effect on pressure of satisfying airfoil boundary conditions at fixed nodes.

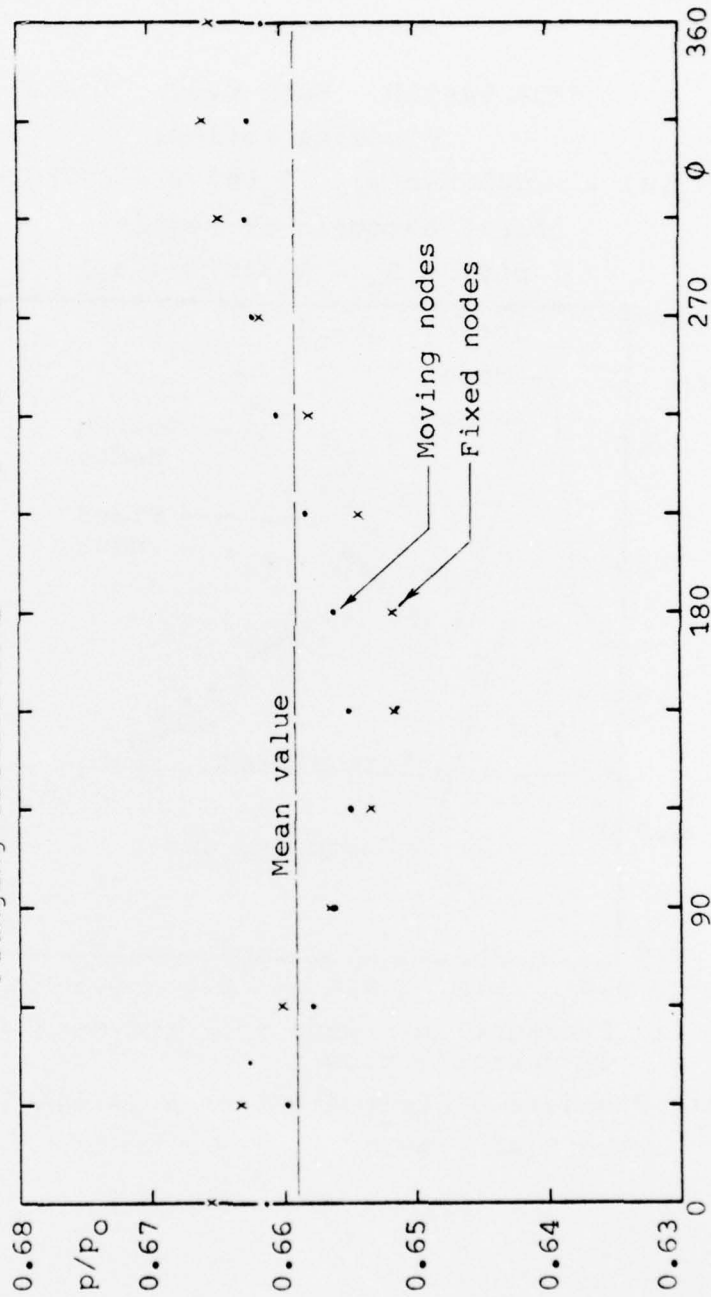
NACA 64A010 . Mach 0.80
 Plunging oscillations $\alpha = 0$ $k = 0.4$



(d) Lower surface, $x/C = 0.66$.

Figure 20. Effect on pressure of satisfying airfoil boundary conditions at fixed nodes.

NACA 64A010 Mach 0.80
 Plunging oscillations $\alpha = 0$ $k = 0.4$



(e) Lower surface, $x/C = 0.82$.

Figure 20. Effect on pressure of satisfying airfoil boundary conditions at fixed nodes.

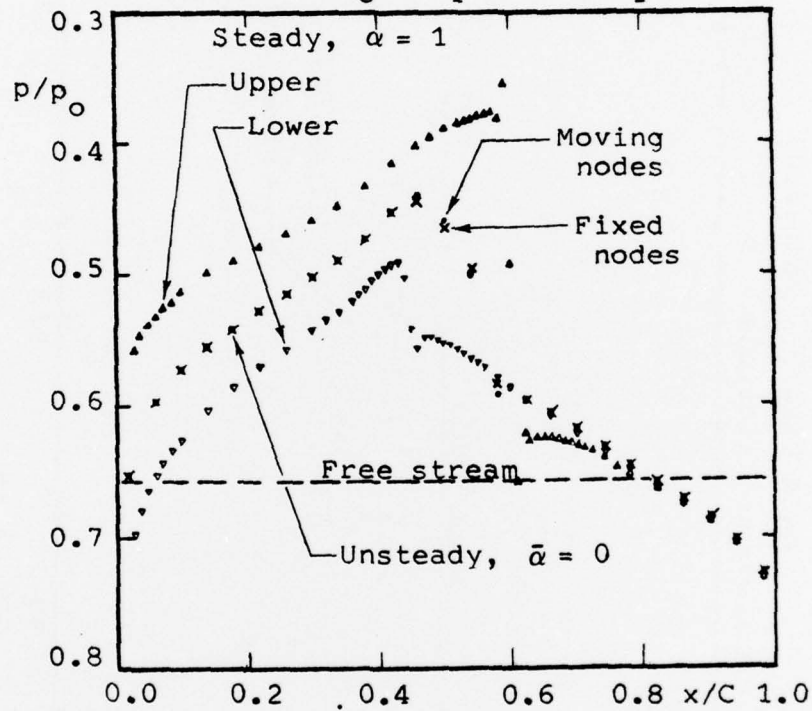
NACA 64A010 Mach 0.80 $\bar{\alpha} = 0$

Plunging motion:

$$y_a(\phi) = -.0436\text{Sin}(\phi) \quad \dot{y}_a(\phi) = -.0175U_\infty\text{Cos}(\phi)$$

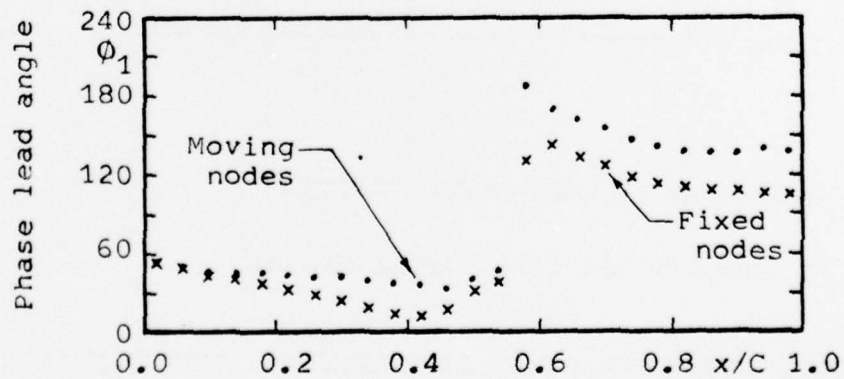
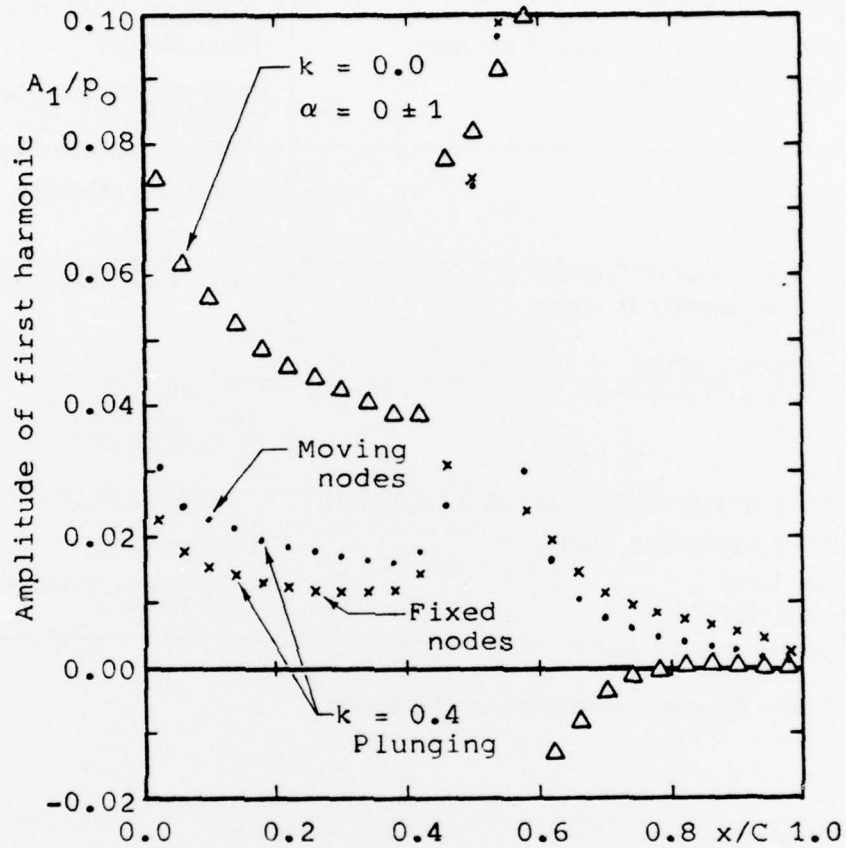
First harmonic of response:

$$p(\phi) = B_0 + A_1\text{Sin}(\phi + \phi_1)$$



(a) Pressure in steady flow and mean value in unsteady flow

Figure 21. Pressure distributions on NACA 64A010 in Mach 0.80 flow.



(b) Amplitudes and phase lead angles of lower surface pressure excursions.

Figure 21. Pressure distributions on NACA 64A010 in Mach 0.80 flow.

REPORT DOCUMENTATION PAGE		READ INSTRUCTIONS BEFORE COMPLETING FORM
1. REPORT NUMBER None	2. GOVT ACCESSION NO.	3. RECIPIENT'S CATALOG NUMBER
4. TITLE (and Subtitle) Computational Research on Inviscid, Unsteady, Transonic Flow Over Airfoils		5. TYPE OF REPORT & PERIOD COVERED Final Report
		6. PERFORMING ORG. REPORT NUMBER CASD/LVP 77-010
7. AUTHOR(s) R. J. Magnus		8. CONTRACT OR GRANT NUMBER(s) N00014-73-C-0294
9. PERFORMING ORGANIZATION NAME AND ADDRESS General Dynamics Convair Division P. O. Box 80847 San Diego, California 92138 406 258		10. PROGRAM ELEMENT, PROJECT, TASK AREA & WORK UNIT NUMBERS
11. CONTROLLING OFFICE NAME AND ADDRESS		12. REPORT DATE January 1977
		13. NUMBER OF PAGES 75
14. MONITORING AGENCY NAME & ADDRESS (if different from Controlling Office) Office of Naval Research (Code 438) Department of the Navy Arlington, Virginia 22217		15. SECURITY CLASS. (of this report) Unclassified
		15a. DECLASSIFICATION/DOWNGRADING SCHEDULE
16. DISTRIBUTION STATEMENT (of this Report) Approved for Public Release, Distribution Unlimited		
17. DISTRIBUTION STATEMENT (of the abstract entered in Block 20, if different from Report) N/A		
18. SUPPLEMENTARY NOTES None		
19. KEY WORDS (Continue on reverse side if necessary and identify by block number) Transonic Airfoil Flow, Unsteady Flow, Finite Difference		
20. ABSTRACT (Continue on reverse side if necessary and identify by block number) The inviscid transonic flow over an NACA 64A410 airfoil oscillating in pitch in a Mach 0.72 stream was calculated with a program based on the unsteady Euler equations. The airfoil oscillates about a mid-chord axis with attitude $\alpha = 1^\circ \pm 1^\circ$ at reduced frequency $k \equiv \omega C/U_\infty = 0.2$. The effects of two approximations made in the analysis, handling of boundary conditions at the airfoil surface and at the perimeter of the computation field, have been studied.		